Nitrate Sorption in the Soils of the Coweeta Hydrologic Laboratory

Patricia Ann Brousseau

Thesis submitted to the faculty of the Virginia Polytechnic Institute and State University
in partial fulfillment of the requirements for the degree of

Master of Science
In
Forestry

B.D. Strahm, Chair
J.D. Knoepp
S.H. Schoenholtz

July 26, 2012
Blacksburg, VA

Keywords: nitrate, sorption, forest soils, oxide, watershed

Nitrate Sorption in the Soils of the Coweeta Hydrologic Laboratory

Patricia Ann Brousseau

ABSTRACT

Atmospheric deposition of reactive nitrogen (N) from anthropogenic sources to forested systems may have acute and long-term deleterious impacts on tree species and water quality. Understanding how nitrate (NO_3^-) moves through the soil system and if it has the potential to be retarded from vertical or lateral leaching allows for a better understanding of the processes important for NO_3^- movement and export from forested watersheds. We examined four watersheds at Coweeta Hydrologic Laboratory (CHL) and determined that soil NO_3^- sorption is a mechanism for abiotic NO_3^- retention. NO_3^- sorption was best described with an S-shaped, sigmoidal model for B horizons that suggests that NO_3^- sorption to soil colloidal surfaces has a higher affinity for soil solution at low equilibrium concentrations. Parameter *a*, the sorption maximum, was most strongly correlated to ammonium oxalate extractable Al (Al_o) and Mn (Mn_o), suggesting that amorphous Al and Mn oxides may be the primary source of positively charged sorption sites. Parameter *b*, the width of the sigmoid curve slope, was best predicted by %C in the soil; suggesting that C compounds may bind to and reduce the availability of positively charged exchange sites for NO_3^- sorption. Previously harvested watersheds exhibited larger variability in parameter values X_o, the inflection point of the curve, and *b*. High elevation watersheds had higher median values for Al_o, Mn_o and the ration of oxalate to dithionite extractable Fe (Fe_o/Fe_d), suggesting that the soils at higher elevations are at earlier stages of pedogenic development and have more poorly crystalline Fe and Al oxides. The greatest potential for sorption maybe at an intermediate soil depth between where there is a significant decrease in biologically cycled C, phosphate and sulfate yet there is enough mineral weathering to provide the mineralogical structures that can support positively charged surfaces.

Table of Contents

1. LITERATURE REVIEW

1.1 Forest Ecosystem N Cycling

1.1.1 Elevated Ecosystem N

Nitrogen (N) is a vital nutrient for life and is limiting to net primary production in most ecosystems. Anthropogenic changes to our natural world have caused major alterations in the N cycle and have resulted in excess N inputs into ecosystems, threatening water quality and species biodiversity (Vitousek et al. 1997). Humans have greatly increased N fixation, the transformation of atmospheric N_2 to biologically available terrestrial forms, from 15 Tg N y^{-1} in 1860 to 156Tg N y^{-1} in 1995 (Galloway et al. 2008). Consequentially, this has resulted in a significant increase in reactive N in terrestrial and aquatic environments.

The advent of anthropogenic N fixation was the discovery of the Haber–Bosch process. The N generated by this process accounts for approximately 80% of the annual flux in anthropogenic reactive N (Gruber & Galloway 2008), which was produced at ten times the rate in 1990 than in 1860 and is projected to continue to increase through 2050 (Galloway 2003). Changes in land management practices, such as the agricultural uses of N fertilizers, have contributed to stream and lake eutrophication (Bouwman et al. 2002). Estuarine and coastal ecosystems have also been profoundly impacted, exhibiting altered function and marine fisheries habitat (Vitousek et al. 1997). Industrial uses of ammonia (NH_3) includes the production of nylons, plastics and animal feed supplements, which make up a smaller percentage of the total use of Haber–Bosch produced N (Galloway et al. 2008). With a growing population, we expect higher agricultural and industrial demands, accelerating reactive N production and use.

Burning of fossil fuels has also significantly contributed to atmospheric reactive N forms including nitrous oxide (N_2O), nitric oxide (NO), and ammonia (NH_3) (Vitousek et al. 1997). These are detrimental to stratospheric ozone and are reduced to nitric acid (HNO_3) in the atmosphere and deposited on earth (Gruber & Galloway 2008). Since the preindustrial era, N deposition has doubled, especially within industrial regions and the northern hemisphere (Green et al. 2004).Although amendments to the U.S. Clean Air Act in 1990 resulted in a cap on sulfur dioxide (SO_2) emissions, there is no legislative policy limiting industrial nitrogen oxide (NO_x) emissions (Driscoll 2001, 2003).

Understanding N cycling within ecosystems is crucial for projecting future impacts of N deposition and ultimately perhaps N saturation; a declining ability of an ecosystem to retain N. This could have a profound effect on soil acidification, stream water quality, and forest productivity (Aber 1992, Vitousek et al. 1996, Driscoll 2003, Palmer et al. 2004). Forested watersheds are of particular interest because they are major contributing areas for water resources and provide vital ecosystem services that include providing timber products and wildlife habitat. Understanding the movement and storage of N within forested catchments is crucial for the assessment of the current and future environmental impacts on the water and vegetative resources produced by these systems.

1.1.2 Paired Forested Watershed Responses to N Deposition

Forested catchments are spatially and temporally dynamic systems and can be highly variable in soil, hydrologic, geologic, climatic, and biotic characteristics. As a result, N fluxes are difficult to predict making the task of defining current and long-term effects of chronic N deposition a challenge (Goodale et al. 2003). For example, in the Harp Lake Watershed, located

approximately 200 km north of Toronto, Ontario, two adjacent watersheds, 10 and 15 ha, with similar vegetation and soils differ in NO_3^- export by a factor of 10 (Schiff et al. 2002). Catchment scale variation in stream NO_3^- concentrations further complicates our ability to define N budgets and pools at the watershed, landscape, and regional scales. At Coweeta Hydrologic Laboratory, a long term USDA Forest Service research station located in the Nantahala Moutains of the Blue Ridge Physiographic Province in southwestern North Carolina, watersheds that differ in elevation, land use, and geology vary in the net difference between NO_3^- input in throughfall and output in stream. These values range from 0.93 kg NO_3^--N $ha^{-1}yr^{-1}$ in formerly clear cut high elevation watersheds to 3.32 kg NO_3^--N $ha^{-1}yr^{-1}$ in high elevation reference watersheds (Swank & Vose 1997). At Hubbard Brook Experimental Forest, a long term USDA Forest Service research station southern White Mountain region of New Hampshire, NO_3^- concentrations within one watershed ranged between 0.01 to greater than 0.2 mgL^{-1} between three streams (Likens & Buso 2006). Therefore understanding patterns in the processes and mechanisms that govern NO_3^- leaching and retention within ecosystems can help foster predictions regarding the variability in stream concentrations. The processes and mechanisms that are important for NO_3^- storage within an ecosystem can help predict how catchments may change with time and inputs. Understanding variability in stream water NO_3^- concentrations at the catchment scale requires an understanding the internal mechanisms that govern processes of interest rather than making inferences based only upon watershed inputs and outputs (Burt & Pinay 2005).

In addition to the observed variability within or across paired watersheds, response to N deposition are also variable across regions. For example, within the Adirondack and Catskill regions of New York, acidic deposition has been negatively impacting forested streams by decreasing pH and acid neutralizing capacity while increasing monomeric Al concentrations

(Driscoll et al. 2004). At the Fernow Experimental Forest in West Virginia, similar results have been found along with an attenuated seasonal variability in NO_3^- export and lower retention of NO_3^- within aggrading forests (Peterjohn et al. 1996). Conversely, watersheds at Hubbard Brook Experimental Forest have been found to have long term declines in NO_3^- export, despite high N deposition rates and aging forests (Goodale et al. 2003); however, the forest is exhibiting the other effects of N deposition such as the leaching of base forming cations from soils and decreases in acid neutralizing capacity in streams (Likens et al. 1996).

1.1.3 Biocycling of N

Biotic assimilation and transformation of N plays an important role in the conversion and translocation of N in forested ecosystems. Many studies have sought to better understand vegetative and soil microbial N cycling within forested ecosystems with the intent of extrapolating these patterns and processes to larger scales (e.g., Nadelhoffer et al. 1984, Ross et al. 2009, Ohrui 1999, Johnson et al. 2000, Fitzhugh et al. 2003 Lui & Muller 1992, Brooks et al. 1996). Within this context, studies have focused on forest ecosystem biotic responses to both N amendments and naturally elevated N scenarios (e.g., Bowden 1991, Fisk & Fahey 2001, Magill et al. 1997, Hultberg et al. 1994, Mitter et al. 1984); however, study approaches are temporally sensitive and greatly vary depending on climatic and vegetative characteristics of the particular study region (e.g., precipitation and stand age). Thus, responses are often variable and inconsistent across studies. For example, Fisk & Fahey (2001) found that net N mineralization, microbial biomass and microbial respiration decreased in response to N amendments at Hubbard Brook Experimental Forest in New Hampshire, whereas at Harvard Forest in central Massachusetts, Magill et al. (1997) found that N amendments increased foliar N, net N mineralization, and net N nitrification.

The microbial and vegetative characteristics of watersheds at Coweeta Hydrologic Laboratory have been studied to better understand ecosystem N availability and losses (Knoepp &Swank 2002, Knoepp & Vose 2007, Knoepp & Swank 1998, Bonito et al. 2003). Climatic factors, temperature and moisture, biotic factors, and C have been found to be factors influencing soil nitrification (Knoepp & Vose 2007). Findings offer insight into potential biotic processes governing NO_3^- production and mobilization within differing landscapes but are difficult to relate directly to NO_3^- export at the catchment scale. Abiotic NO_3^- retention may be a mechanism for the retardation of NO_3^- from leaching to ground water, which could offer insight into variation in stream NO_3^- export between watersheds.

1.2. Abiotic N Sorption

1.2.1 Dissolved Organic Species

Much of the soil N cycling research conducted to date has been focused on surficial biotic soil dynamics and vegetative retention; few have attempted to understand abiotic N retention mechanisms and how these processes may differ spatially within a forested watershed. Upper portions of the soil profile act as source regions for dissolved inorganic and organic forms of N. It is also where readily available forms of N are predominantly taken up by fine roots and assimilated within microbial biomass. Inorganic and organic N, along with dissolved organic carbon (DOC), not utilized in the upper portions of the soil profile are subject to leaching and subsequent retention on soil colloids deeper in the soil profile. Studies in glaciated regions of the northeastern USA have proposed abiotic retention of dissolved N constituents within the mineral soil in forested catchments as important (Fitzhugh et al. 2003, Dittman et al. 2007), although little is known about the mechanism. At the Coweeta Hydrologic Laboratory, Qualls et al. (2002) found that a large percentage of the DOC and N leached from O horizons were removed within

the A and B horizons as a result of DOC being adsorbed to Fe and Al oxyhydroxides. They concluded that retention mechanisms for inorganic nutrients and the adsorption of DOC prevented leaching of soluble soil solution constituents (Qualls et al. 2002).

1.2.2 Sorption of NO_3^-

Following the decomposition of plant and organic residues, mineralization of organic matter produces ammonium (NH_4^+). This can then be oxidized to NO_3^- through the microbial mediated process of nitrification. NO_3^- has various fates once in soil solution. It can be leached, denitrified back to N_2, taken up by plant roots, assimilated in microbial biomass, or sorbed to soil colloidal surfaces. Sorption has been shown as a mechanism for NO_3^- retention in studies involving highly weathered argillic horizons from Oxisols and Ultisols (Cahn et al. 1992, Eick et al. 1999) and soils with volcanically derived parent materials (Tani et al. 2002, Strahm & Harrison 2006). Generally, studies have found sorption to increase with soil depth and decrease with organic matter content.

Mechanistically, these studies differ from those that have suggested that abiotic retention occurs through the incorporation of NO_3^- into soil organic matter (Dail et al. 2001, Davidson et al. 2003), around which there is debate and uncertainty over the mechanism leading to the observed abiotic retention of NO_3^- (Coleman et al. 2007). The general hypothesis for the incorporation of for this abiotic NO_3^- retention mechanism, known as the ferrous wheel hypothesis, is the reduction of NO_3^- to nitrite (NO_2^-) through the oxidation of Fe(II) to Fe(III). NO_2^- resulting from this reaction then is proposed to interact with dissolved organic matter (DOM) to produce dissolved organic N (DON). By contrast, abiotic sorption proposed in this study involves an electrostatic, non-covalent interaction while the ferrous wheel hypothesis

requires thermodynamically favorable conditions for a specific oxidation-reduction reaction to occur and subsequent covalent bonding with DOM.

The ability for weathered soils to adsorb NO_3^- increases with depth, oxide abundance, and NO_3^- concentration and with decreases in pH, soil organic matter content and competing anion concentrations (Johnson & Todd 1983,Eick et al. 1999, Alves & Lavorenti 2004, Black & Waring 1976, Toner et al. 1989, Wong et al. 1990, Cahn et al. 1992). The pH of the soil is a measure of the presence of H^+ and therefore the potential to create positive sorption sites on certain soil minerals (Back & Waring 1976). Total C serves as an indicator of soil organic matter which can cover, or preferentially bind to, positive exchange sites in variable-charge soils (Xu et al. 2005, Stahm & Harrison 2008). Inorganic sulfur in the form of sulfate (SO_4^{2-}) is an anion that can compete with NO_3^- for positively charged exchange sites and can serve as an indicator of anion competition (Essington 2004).

Although the total NO_3^- sorbed may be minimal in comparison to the total inorganic and organic N pool within a soil ecosystem, the total NO_3^- sorbed relative to the NO_3^- leached maybe substantial. Within Andisols in the Pacific Northwestern USA, Strahm and Harrison (2006) found that the percent of NO_3^- sorbed relative to NO_3^- leached in a harvested and uncut stand was 67% and 170%, respectively. Nitrate sorption can serve as a significant phenomenon to retain mobile N and may profoundly influence stream water NO_3^- concentrations.

1.2.3 Metal Oxides

Metal oxides are weathering products of primary and secondary minerals and can profoundly affect soil colloid and solution chemistry (Essington 2007). Metals such as Fe, Al, and Mn are weathered from layer silicates precipitate into the form of hydrous oxides, hydroxides, and oxyhydroxides, collectively known as oxides. They are often found in

association with the minerals from which they were derived and have the potential to coat the surfaces of layer silicate clays, potentially inhibiting their interaction with dissolved constituents in soil solution. Metal oxides have large, highly reactive surface areas that can form surface complexes with ligands, metals and molecular species.

The potential for mineral soils to have variable charge and possess positive exchange sites is dependent on the type of metal oxide present and the pH of the soil environment. Metal oxides occur within soils as a continuum of crystalline, paracrystalline, and amorphous forms (Essington 2004). The more crystalline metal oxides, referring to the extent of ordered stacking in hydroxide layers, have less reactive surface area than amorphous forms and therefore have fewer potential surface reactions and exchanges with the soil solution relative to more amorphous forms. Gibbsite (γ-Al $(OH)_3$) is fairly ubiquitous in weathered soils and is poorly crystalline. Gibbsite is highly reactive with single coordinating edges and has been found to bear a positive net charge when soil pH < 9 (Essington 2004). Iron oxides tend to have a greater number of forms that have a higher range in structure. The more crystalline structures, goethite (α-FeOOH) and hematite (α-Fe_2O_3), are commonly found in temperate and tropical climates, respectively. Ferrihydrite (Fe_5HO_8*$4H_2O$) has a less crystalline structure and is commonly found in association with hematite in tropical climates. Although some isomorphic substitution can occur within Fe-oxides, the net surface charge, positive or negative, depends on the pH of the soil solution (Essington 2004, Toner et al. 1989, Eick et al. 1999). In addition to the abundance of exchange sites, the soil solution needs to be acidic in order for hydrogen (H+) to bind to exchange site hydroxyl groups and create the positively charged exchange microsites necessary for anion adsorption.

1.2.4 Selective Dissolution Analysis

As discussed, there are many defined forms of metal oxides that occur in the soil environment as a continuum from crystalline to amorphous forms. Chemical dissolution procedures target operationally defined fractions of metal oxides so that general information regarding their abundance and structure can be obtained. Although they do not identify specific minerals directly, these methods are relatively simple and have been employed in many studies (Jackson et al. 1986, Parfitt & Childs 1988). The three dissolution techniques generally used for extracting operationally defined Fe, Al, Si and Mn oxide fractions in soils are sodium pyrophosphate, acid ammonium-oxalate, and dithionite-citrate bicarbonate (Jackson et al. 1986, Parfitt & Childs 1988). These procedures are part of the spatially explicit databases (e.g., STATSGO2) as part of the Natural Resources Conservation Services (NRCS) State Soil Geographic database. Sodium pyrophosphate has been shown to predominantly extract Fe and Al associated with organic matter (Loveland and Digby 1984). Aluminum associated with organic matter tends to be monomeric or in hydroxyl polymer form (Parfitt & Childs 1988). However Fe associated with organic matter tends to be amorphous Fe structures such as goethite and ferrihydrite (Fe_2O_3* 0.5 H_2O) (Parfitt & Childs 1988). Acid ammonium-oxalate also extracts the same fractions as pyrophosphate with the exception of goethite, which poorly reacts with acid-oxalate (Parfitt & Childs 1988, Bera et al. 2005). Additionally acid ammonium-oxalate also extracts amorphous Fe and Al oxides such as allophone, imogolite, and gibbsite (Parfitt & Childs 1988, Essington 2004). Dithionite-citrate bicarbonate extracts both non-crystalline and crystalline forms of oxides, including hematite, goethite and ferrihydrite (Parfitt & Childs 1988).

1.2.5 Landscape Variability in Soil Weathering

Pedogenic variation at the catchment scale can provide insight into how hydrous metal oxides vary within and between watersheds. Soil development is an anisotropic process,

including both vertical and lateral pedogenic processes, such as the elluviation and illuviation of clays and organic matter, dissolution and precipitation reactions, etc. These processes differ spatially depending on hillslope topographic position, parent material, elevation, aspect, as well as biotic factors (Park & Burt 2002). Using soil series to identify variations in soil attributes can be a way of identifying characteristics of interest, such as oxide abundance and composition. Soil series are also mapped based upon topographic and climatic factors which allows for the identification of specific regions of interest that may be functionally similar in biogeochemical processes. Catchment spatial variation in soil forming factors and hydrology create variation in soil pedogenesis and thus provide insight into weathering processes important for the development of hydrous metal oxides that may lead to the sorptive retention of NO_3^-.

2. INTRODUCTION

Nitrogen (N) is a vital nutrient for life and limits net primary production in most terrestrial and aquatic ecosystems. Anthropogenic N sources, such as inorganic fertilizers and the burning of fossil fuels, have caused major alterations in the global N cycle resulting in excess N inputs to ecosystems, threatening water quality and species biodiversity (Vitousek et al. 1997). Understanding N cycling within ecosystems is crucial for projecting future impacts on the ability of terrestrial ecosystems to retain N which in turn affects soil acidification and fertility, forest productivity, and stream water quality (Aber 1992, Vitousek et al. 1996, Driscoll 2003, Palmer et al. 2004). Forested watersheds are of particular interest because they are major contributing areas for water resources and sources of forest products. Atmospheric N deposition and forest management practices may cause an increase in the generation and export of soluble forms of N, particularly nitrate (NO_3^-). Understanding the movement and storage of N within forested

catchments is important for assessing current and future environmental impacts on the water and vegetative resources produced by these systems.

Forested catchments are spatially and temporally dynamic systems and as such, are highly variable in soil, hydrologic, geologic, climatic, and biotic characteristics. As a result, soil and stream water N fluxes are difficult to predict and fully understand (Goodale et al. 2003). Catchment scale variation in stream NO_3^- concentrations further complicates our ability to define the N outputs at watershed and regional scales. Understanding variability in stream water NO_3^- concentrations at the catchment scale requires the investigation of internal N cycling mechanisms that govern soluble N fluxes rather than making inferences based solely upon watershed fluxes (Burt & Pinay 2005).

In an effort to understand internal watershed N cycling, many studies have focused on biotic (i.e., vegetative and soil microbial) N processes within forested ecosystems with the goal of extrapolating the observed patterns and processes to larger spatial scales (e.g., Nadelhoffer et al. 1984, Ross et al. 2009, Ohrui 1999, Johnson et al. 2000, Fitzhugh et al. 2003, Lui & Muller 1992, Brooks et al. 1996). Research studies have also focused on forest ecosystem biotic responses to both N amendments and naturally elevated N deposition (e.g., Bowden 1991, Fisk & Fahey 2001, Magill et al. 1997, Hultberg et al. 1994, Mitter et al. 1984). Results of both lines of research show N cycling is temporally and spatially variable and sensitive to the biogeoclimatic characteristics of the particular study region (e.g., precipitation and stand age) at any particular time. Thus, responses are often variable and inconsistent and obscure our ability to explain N cycling and export beyond specific regions.

Less studied are the abiotic sorption and desorption reactions that have been shown as a mechanism for NO_3^- retention in studies involving highly weathered Oxisols and Ultisols (Cahn

et al. 1992, Eick et al. 1999), volcanically derived Andisols (Tani et al. 2002), and other soils with andic soil properties (Strahm & Harrison 2006, 2007). Mechanistically, these studies vary from the suggested abiotic retention that has been observed through the incorporation of NO_3^- into soil organic matter (Dail et al. 2001, Davidson et al. 2003) and should be separated from the debate and uncertainty of those observations (Coleman et al. 2007).

The ability for a soil to sorb NO_3^- from soil solution is dependent on the development of positive charge on the surfaces of mineral soil colloids. Specifically, NO_3^- sorption refers to outer-sphere, electrostatically maintained adsorption and does not include covalent bonding with mineral surfaces. This type of sorption tends to increase with soil acidity and the abundance and composition of hydrous metal oxides and decrease with soil organic matter content and the presence of competing anions (Johnson & Todd 1983,Eick et al. 1999, Alves & Lavorenti 2004, Black & Waring 1976, Toner et al. 1989, Wong et al. 1990, Cahn et al. 1992, Strahm and Harrison 2007). Many hydrous metal oxides, especially those with poorly crystalline or amorphous structures, have highly reactive surfaces that can develop either positive or negative charge depending upon the pH of the soil system (Essington 2004). Although most bulk soils have a net negative charge, the influence of positively charged colloidal microsites can lead to significant sorption of NO_3^- (Toner et al. 1989, Cahn et al. 1992, Eick et al. 1999, Strahm and Harrison 2006, 2007). Nitrate sorption has been studied in agricultural systems due to the importance of N for crop production and environmental issues associated with N leaching (Black & Waring 1976, Toner et al. 1989, Wong et al. 1990, Cahn et al. 1992, Eick et al. 1999). Less work in this area has been done in forest systems (Strahm & Harrison 2006, 2007, Kimsey et al. 2011) that are generally more acidic and have minimal soil nutrient amendments. Using soils from paired watersheds at Coweeta Hydrologic Laboratory (CHL), our objective for this study

was to determine if NO_3^- sorption is a potential mechanism for abiotic NO_3^- retention. This can help in the prediction of previously observed differences in watershed scale NO_3^- export. We will address this by developing predictive relationships between soil chemical properties and NO_3^- sorption parameters for genetic soil mineral horizons in four watersheds with differing site use histories, as well as different soil chemical and stream N export characteristics.

3. METHODS

3.1. Site Description

This study took place at the USDA Forest Service, Coweeta Hydrologic Laboratory (CHL), an experimental forest located in the Nantahala Mountains of the Blue Ridge Physiographic Province in southwestern North Carolina (Figure 1). Annual precipitation is approximately 1900 mm and ranged from 1800mm at low elevation and 2500mm at high elevations with monthly precipitation generally greater than 100 mm (Swank and Vose 1997). Monthly temperatures peak during June through August (~20°C) and are minimal from December through January (~5°C) (Knoepp et al. 2007). Generally, the vegetative species found at CHL are oaks and mixed hardwoods. In addition to *Quercus* spp. (oaks), this includes *Carya* spp. (hickory), *Nyssa sylvatica* (black gum), *Liriodendron tulipifera* (yellow poplar), and *Tsuga canadensis* (eastern hemlock). The understory species are mainly *Rhododendron maximum* (rhododendron) and *Kalmia latifolia* (mountain laurel) (Day et al. 1988).

We selected paired watersheds (reference and disturbed) from across an N deposition gradient within CHL to evaluate the relative importance of N loading and land use history on the potential for the soils of the CHL to sorb NO_3^-. In both watershed pairs, the disturbed watershed has significantly greater stream NO3concentrations and reference watersheds show increasing

relative annual flow weighted NO_3^- concentrations which has been attributed to both increases in atmospheric N deposition and forest maturation, although concentrations are low and frequently at or near detection limits (Swank & Vose 1997). Additionally, the seasonal duration and amplitude of NO_3^- in streams have increased. High elevation streams have higher NO_3^- concentrations and twice the positive rate of change in stream NO_3^- than lower elevation watersheds. For all watersheds, stream NH_4^+ concentrations were low and temporally invariable (Swank & Vose 1997).

Watersheds 36 and 37 are high elevation (1021-1585 m), east facing catchments (Figure 1). Watershed 36 (49 ha), the high elevation reference watershed (RH), was partially defoliated from fall cankerworm from 1975 to 1979. Watershed 37 (44 ha), the disturbed high elevation watershed (DH), had all woody vegetation cut and left on site in 1963. Watersheds 2 and 7 are lower elevation (701– 1006 m) south facing catchments. Watershed 2 (12 ha) is the reference low elevation watershed (RL) and has been undisturbed since 1927. Watershed 7 (59 ha) was the disturbed low elevation watershed (DL) and was grazed by cattle from 1941 to 1952 and commercially clear-cut using cable-yarding techniques in 1977 (Figures 1 & 2).

The soils of CHL are weathered from felsic and mafic igneous and high-grade metamorphic rocks including granite, hornblende gneiss, granodiorite, biotite gneiss, and high grade metagraywacke (Soil Survey Staff, 2010). The Shope Fork Fault runs through the center of the Coweeta basin defining a break between the Otto and the Coweeta Group Formations. The Coweeta Group consists of three lithostratigraphic regions; the Coleman River formation, the Persimmon Creek Gneiss, and the Ridgepole Mountain Formation. Watershed 37 and half of watershed 36 are part of the Coleman River formation which consists of metasandstone and quartz feldspar gneiss with subordinate amounts of interlayered pelitic schists and calc-silicate

quartzite (Hatcher 1988). The Otto formation, located in the northern regions of the basin (Watersheds 2, 7, and the rest of 36), is comprised of sedimentary protoliths of low compositional maturity and is mostly biotite paragneiss and biotite schist (Hatcher 1980, 1988).

Soils of CHL are mapped as Inceptisols and Ultisols (Soil Survey Staff, 2010). High elevation watersheds 36 and 37 are composed of variations of Dystrochrepts that differ primarily in the thickness of the A and Bw horizons. Near stream, south facing slopes tend to be dominated by the Cullasaja (loamy-skeletal, isotic, mesic Humic Dystrudepts) and Tuckasegee (fine-loamy, isotic, mesic Humic Dystrudepts) complex that are formed in colluvium and have thick, very dark, A horizons. Mid-slope positions are mapped as the Edneyville series (coarse-loamy, mixed, active, mesic Typic Dystrudepts) and have smaller A-horizon and thicker Bw horizons than the near stream zone. Upper slope positions, close to the watershed divide, tend to be of the Rock outcrop-Cleveland complex and Wayah (fine-loamy, isotic, frigid Humic Dystrudepts) soil series. The Cleveland series (loamy, mixed, active, mesic Lithic Dystrudepts) exists on steep slopes, 50-90 percent, and tend to be shallow. The Wayah series is a deeper soil with a large A-horizon and usually associated with summit ridge positions. North facing slopes are generally dominated by the Plott series (fine-loamy, isotic, mesic Humic Dystrudepts). Low elevation watersheds 2 and 7 are mapped as Typic Hapludults and Typic Dystrochrepts, with the near stream positions mapped as the Cullasaja-Tuckasegee complex. Mid-slope positions are dominated by the Fannin series (fine-loamy, paramicaceous, mesic Typic Hapludults) and are characterized by very shallow A-horizon and one to two Bt horizons. At higher locations within watershed 7 there is the Chandler series (coarse-loamy, micaceous, mesic Typic Dystrudept) which are shallower soils than the Fannin series and the Cullasaja-Tuckasegee complex.

3.2 Soil Sampling

Forty-two sampling points were located within the four watersheds (Figure 2). Based on watershed area, Watersheds 7, 36, and 37 each have 12 points and WS 2 has 6 points. Sampling points were distributed across the watersheds to maximize spatial variability of soil, vegetation, and climatic factors. The elevation of each plot was quantified using ArcGis and a 10m digital elevation model. In March 2011, a composite sample of each genetic soil horizon to 1 m was collected from four locations at each sampling point. Subsample locations were approximately 5 m to the N, S, E and W of the sampling point. The depth and thickness of each horizon was recorded from a single quantitative soil pit located at each point. Soil horizon depths were quantified as the depth in cm from the top of the forest floor-mineral soil interface to the top of the soil horizon. A total of 120 soil horizons were collected, air-dried, and passed through 2mm sieve before chemical analysis.

3.3 NO_3^- Sorption

Isotherms were developed using batch equilibration techniques on bulk soil samples following the methods of Strahm and Harrison (2006, 2007) where 2.5 g of air dried soil was placed into 30 ml polyethylene centrifuge tubes. Soils were combined with six known concentrations of NO_3^- (5, 2.5, 1.25, 0.625, 0.3125, and 0 mmol L^{-1}) in the form of $NaNO_3$ at a 1:4 soil to solution ratio. Three drops of toluene were added to each tube to prevent biologically mediated N transformations. Each soil horizon was combined with each NO_3^- concentration once. Tubes were shaken for one hour on a reciprocal shaker. Samples were centrifuged for 15 min at a force of 1050*g* and the supernatant was decanted into scintillation vials. Initial residual NO_3^- in B horizons soil samples was extracted using 2M KCl. The solutions were analyzed for NO_3^- on a Bran+Luebbe TRAACS 2000 AutoAnalyzer using an imidazole buffer; which has been found to be less sensitive to solution Fe interference than the ammonium chloride EDTA

method (Coleman et al. 2007). Additionally, background Fe concentrations averaged 0.50 mg Fe L^{-1}, well below the concentrations in which Coleman et al. (2007) found Fe to interfere with NO_3^- detection.

Following the batch equilibration method, NO_3^- adsorption was calculated as:

$$q\ (mmol\ NO_3^-\ kg^{-1}) = V_l((C_{in}+C_i)-C_{out}))/m_s \qquad (eq1)$$

Where q is the quantity of NO_3^- sorbed per unit soil, m_s is the mass of air dried soil (kg), and V_l is the volume of solution (L). C_{in} and C_{out} represent NO_3^- solution concentrations (mmol L^{-1}) before and after batch equilibrium techniques are employed. Variable C_i represents the initial NO_3^- concentrations in the soil samples before the batch equilibrium techniques were employed. Data was graphed using the q as the response variable and C_{eq} (equilibrium solution NO_3^- concentration), which is C_{out}, as the predictor variable. Since A-horizon soils did not have the initial NO_3^- concentrations accounted for when generating q values, therefore NO_3^- adsorption was calculated as;

$$q\ (mmol\ NO_3^-\ Kg^{-1}) = V_l(C_{in}-C_{out})/m_s \qquad (eq2)$$

3.4 Sorption Isotherms

Using q as the dependent variable and C_{out} as the independent variable, multiple Langmuir and Freundlich isotherm equations were used to fit curves to the experimental data in order to derive curve-fitting parameters (MATLAB) that could then be related to soil properties. For the Langmuir model, these parameters include the slope of the isotherm as q approaches zero (abbreviated as b) and the maximum value that q approaches as the equilibrium concentration becomes large (abbreviated as N_{max}). The Freundlich model includes a parameter describing the degree of inflection (N) and a constant K. Additionally, hybrid models of Langmuir and Freundlich, (Hinz 2001) were tested to find the best model fit that can be applied to each genetic

soil horizons. The model choice was based upon the overall goodness of fit for all B horizons with each model and determined by estimating the median standardized confidence interval [SCI= ($CI_{upper} - CI_{lower}$)/parameter value] for each parameter. The equilibrium concentration (C_{eq}) threshold at which NO_3^- sorption begins was calculated as C_{eq} (mmol $NO_3^- L^{-1}$) = X_o - 1/2(b).

3.5 Soil Chemical Analyses

Selective dissolution analyses were used to determine the relative amounts of extractable Fe, Al, Si, and Mn for each sample. Different selective dissolution extractions represent different oxide forms and are used as indices of the availability of NO3 sorption sites. We determined sodium pyrophosphate and dithionite-citrate bicarbonate extractable fractions of Fe, Al, Si, and Mn using methods from the NRCS Soil Survey Laboratory Methods Manual (2004). The sodium pyrophosphate extraction was performed using 0.1 *M* $Na_4P_2O_7 \cdot 10H_2O$ at a pH of 10. In 100 ml polyethylene centrifuge bottles, 0.5 g of soil was combined with 30ml of sodium pyrophosphate solution and shaken for 12-16 h on a reciprocal shaker at 200 oscillations min^{-1}. After samples were shaken they were left to sit for another 16 hours and then centrifuged at 1050*g* for 15 min. Metals extracted with sodium pyrophosphate will be defined as M_p.

The dithionite-citrate bicarbonate extraction was performed using 0.57 *M* sodium citrate dihydrate ($Na_3C_6H_50_7 \cdot 2H_2O$) and sodium dithionite ($Na_2S_2O_4$) purified powder. In 100 ml polyethylene centrifuge bottles 0.75 g of soil was combined with 30 ml of sodium citrate solution and 0.4 g of sodium dithionite purified powder using a calibrate scoop. Samples were shaken for 12-16 h on a reciprocal shaker at 200 oscillations min^{-1}. After samples were shaken they were left to sit for approximately 12 of hours and centrifuged at 1050*g* for 15 min. Metals extracted with dithionite-citrate bicarbonate will be defined as M_d.

The acid oxalate extraction was performed using methods from Jackson et al. (1986) and Parfitt and Childs (1988) in a solution containing 0.2 *M* ammonium oxalate ($C_2H_8N_2O_4 \cdot H_2O$) and 0.2 *M* oxalic acid ($C_2H_2O_4 \cdot 2H_2O$); solutions were made and kept in the dark. In 100 ml polyethylene centrifuge bottle wrapped in aluminum foil, 0.5 g of soil was combined with 50 ml acid-oxalate solution. Samples were shaken for 4 h on a reciprocal shaken at 200 oscillations min^{-1} and centrifuged at a force of 1050*g* for 15 min. Metals extracted with ammonium oxalate will be defined as M_o.

Following centrifugation in each selective dissolution analysis, supernatants were decanted and filtered through Whatman No. 40 filter paper and frozen until subsequent analysis on a Varian Vista MPX ICP-OES. Data from the various fractions were used to calculate various ratios to provide alternative metrics that could provide additional information.

Additional chemical analyses included phosphate extractable sulfate (S_{CaPO4}), total C and N, and pH. Sulfate is a potential competing anion, representing an inorganic and exchangeable form of S, and was determined using the methods of Fox and Olsen (1964), Anderson et al. (1992) and Gustafsson & Jacks (1992). The extraction was performed using 0.01 *M* $Ca(H_2PO_4)_2$ and adjusting the pH to 4 through the addition of H_2PO_4. In 100 ml polyethylene centrifuge bottles, 5 g of each soil sample was combined with 50 ml of $Ca(H_2PO_4)_2$ solution and mixed on a reciprocal shaker for 1 h at 200 oscillations min^{-1}. Samples were then centrifuged for 15 min at a force of 1050*g* and filtered using Whatman No. 40 filter paper before being analyzed on a Varian Vista MPX ICP-OES for total S. Total C and N were determined by combustion on dry soils using an Elementar Vario MAX CNS. The pH was determined in a 1:1 ratio of soil:distilled water and allowed to equilibrate for 2 h prior to measurement using a Thermo Orion model 8165BNWP Ross combination electrode.

3.6 Statistical Analysis

Statistics were calculated using Minitab 16 Statistical Software. Median and upper 75 % and lower 25% quartile values of sorption parameters and soil characteristics for each watershed were calculated. Correlation coefficients were determined between soil characteristics and sorption isotherm parameter values using Spearman's nonparametric correlation with untransformed data.

Multiple regression models were created using soil characteristics to predict sorption isotherm parameters. Isotherm parameters were weighted based upon the RMSE, root mean square error, from the model fit determined during the curve fitting and parameter generation in order to account for the error in the original model fits. The need for data transformations was determined using deleted (studentized) residuals plotted for each parameter against each predictor variable. Oxalate extractable Al_o and Mn_o as well as the % C received logarithmic transformation to yield a semi-normal distribution. Mn_o:Mn_d received a square root transformation. Initial models were reduced depending upon the significance of each variable according to t-tests ($\alpha < 0.1$), Mallows Cp tests and variance inflation factors. Outliers were identified as leverage points, extreme predictor values that have the potential to influence the regression fit, by using Hi tests and were visually observed on deleted residual vs. individual predictor plots. Cook's distance and DFITS , diagnostics to determine how influential a particular point is in a regression, use both unusual predictors and residuals, unusual Y values, to determine high influence points.

4. RESULTS

4.1 NO_3^- Sorption Isotherms

A-horizons soils showed little evidence of NO_3^- sorption. Most A-horizons exhibited small and inconsistent levels of sorption that did not fit any of the sorption isotherm models used in this study. The quantity sorbed (q) was minimal for most of the equilibrium solution concentrations. Due to the lack of quantifiable sorption the A horizons were eliminated from subsequent analysis (Figure 3).

The Freundlich, Langmuir, and hybrid sorption isotherm models were not universally applicable to the sorption data. However, an S-shaped model proved to be the best fit for the isotherm data for most B horizon soils (Figure 4). The model equation used for the S-shaped isotherm is a three parameter, sigmoid, logistic model defined as:

$$q\ (mmol\ NO_3^-\ kg^{-1}\ soil) = a/(1+exp(-(C_{eq}(mmol\ NO_3^-\ L^{-1})-X_o)/b) \qquad (eq\ 3)$$

where q is the quantity of NO_3^- sorbed per unit soil, C_{eq} is the solution equilibrium concentration, a represents the theoretical sorptive maximum, X_o defines the equilibrium concentration at half of the maximum value (y = a/2), and b describes the width of the sigmoidal curve so that as b approaches zero, the resulting curve looks like a step function. Therefore b describes the abruptness rapidity of sorption prior to saturation (Meyer et al. 1999, Uribe and Martin 2007).

Of the 65 B horizons isotherms, 57 fit to the sigmoid model and were used in the subsequent statistical analyses. The median standardized difference between upper and lower confidence intervals for the parameters a, X_o and b were 0.35, 0.43, and 1.19, respectively. The median R^2 value was 99.2%.

The three model parameters were used as the response variables for multiple regression analyses and correlations with soil characteristics. Among the sorption isotherm parameters, the strongest correlation was between parameters *b* and X_o ($r = 0.71$, $p < 0.00$). Parameters *a* and *b* ($r = 0.55$, $p < 0.00$) and X_o ($r = 0.53$, $p < 0.00$) are positively correlated suggesting that higher sorption maximums require a higher equilibrium concentration to reach it and sorption is more gradual. Values of the equilibrium concentration (C_{eq}) at which NO_3^- sorption begins ranged from 0.59 to 3.93 mmol NO_3^- L^{-1}.

4.2 Soil Properties and Sorption Isotherm Parameters

Table 1 shows Spearman's correlation coefficients and p-values for the correlations between soil properties and isotherm parameters. Parameter *a* is positively related to S_{CaPO4} and to all extractable Fe and Al from the selective dissolution analysis. Similar positive correlations were observed with extractable Mn, with the exception of Mn_d. Parameters *b* and X_o had significant correlations with most of the same soil characteristics as each other, including %C [b ($r = 0.28$) and X_o ($r = 0.32$)] and pH [b ($r = -0.24$) and X_o ($r = -0.38$)]. The strongest correlations for parameters X_o and *b* with selective dissolution analyses were Al_o and Mn_o and Mn_p (Table 1).

4.3 Multiple Regression Models

Multiple regression models were used to determine if a combination of multiple soil properties could explain the variation in each parameter. Parameter *a* was explained by the model below ($R^2 = 0.445$):

$$a = 0.414 + 0.239\ log\ \%\ Al_o + 0.00698\ depth + 0.212\ sqrt\ Mn_o/Mn_d \quad (eq4)$$

Parameter *b* was best predicted singularly by the %C with an R^2 of 0.678.

$$b = 0.415 + 0.140\ log\ \%C \quad (eq5)$$

The multiple regression model for X_o included the S_{CaPO4}, the % Al from the ammonium oxalate extraction and %C. The R^2 was 0.38.

$$X_0 = 2.25 - 0.246\ S_{CaPO4} - 0.219\ log\ \%C + 0.636\ log\ \%Al_o \quad (eq6)$$

4.4 Watershed Variability

Disturbed watersheds, at both high and low elevations, show greater variability in *b* and X_o NO3 sorption isotherm parameters with larger upper and lower quartiles and distribution of values than reference watersheds (Figure 5). Conversely, *a* did not show differences in variation between reference and disturbed watersheds but tended to increase with elevation. Parameter *a* also exhibited the largest values in the high elevation disturbed watershed (DH) and the distribution of data was skewed to the right (Figure 5). Within all the watersheds, B2 horizons (including both Bw2 and Bt2 horizons) tended to have a higher sorption maximum than upper B horizons (Figure 4).

Soil C tends to increase while pH tends to decrease with elevation (Table 3) and C and pH are negatively correlated (Table 2). High elevation watersheds tended to have the highest Al_p, Fe_p, Al_o, and Fe_o as well as the greatest ratio of Fe_o/Fe_d (Table 3). This is particularly true of the disturbed high elevation watershed, whose 25% quartiles do not overlap with the 75% quartiles from the lower elevation median values for these fractions. Mn_o and Mn_d tended to be higher within the high elevation watersheds however the 25% quartile of the median values overlapped with the upper 75% quartile values of the lower watersheds median values (Table 3).

5. DISCUSSION

5.1 Sorption Isotherms

Although sorption did occur at higher solution equilibrium concentrations within some A-horizons, many of the sorption values were negative (Figure 3) suggesting that NO_3^- was moving into soil solution rather than being sorbed to mineral surfaces or incorporated into organic matter. The lack of sorption within some A-horizons could be a result of organic matter coatings on positively charged mineral surfaces. Qualls et al. 2002 observed rapid adsorption of DOC in A-horizon soils at CHL. There may be a potential for abiotic NO_3^- sorption in A-horizons, due to the presence of Fe and Al oxides, however C is prohibiting NO_3^- from sorbing. Poor SO_4^{2-}sorption in surface horizons due to organic carbon was also observed in Johnson & Todd (1983).

The S-shaped curve of the NO_3^- sorption isotherms suggests that at lower equilibrium concentrations, NO_3^- has a higher affinity for soil solution than for soil colloidal surfaces (Essington 2004) (Figure 4). This could indicate the presence of competing anions (e.g., sulfate, phosphate, organic anions) preventing NO_3^- sorption to colloidal surfaces, or NO_3^- having a higher affinity for interaction with other solutes in soil solution (e.g., Al^{+3}). After a certain concentration, the affinity of NO_3^- for sorption to soil colloidal surfaces increased. At higher NO_3^- concentrations, the curve tended to plateau, indicating a saturation of sorption sites (Grant et al. 1998, Meyer et al. 1999) that varied by watershed, elevation, and disturbance regime (Figure 4).

The S-shape of the NO_3^- sorption isotherms in this study are atypical; a L-shaped curve, characterized by the Langmuir isotherm, tends to be more commonly observed in anion sorption

(Eick et al. 1999, Cahn et al. 1992, Strahm & Harrison 2006, Kimsey et al. 2011) The sigmoidal, three parameter model we used is not commonly used to describe NO_3^- sorption. We cannot explain why this occurs using the data collected for this study. It may be related to the ionic strength of the soil solution at the time in which the samples were collected. The samples were retrieved after a storm event that resulted in approximately 7.6 in of precipitation. After drying and rewetting the soil samples, the ionic strength of the soil solution could have been very low resulting in NO_3^- having a higher affinity to soil solution. Conversely, there could have been a higher abundance of dissolved Fe and Al in the soil samples that could also create an attraction of NO_3^- to soil solution. It is unclear however the data collected for this study suggests a possible temporal or spatial sensitivity of this mechanism.

Although NO3 sorption is a theoretically plausible phenomenon at certain equilibrium concentrations, it's relevance in the ecosystem is questionable without a better understanding of the driver behind the S-shaped isotherm. Sorption was initiated at a median C_{eq} value of 1.418 mmol NO3 L^{-1} and ranged between 0.59 mmol L^{-1} and 2.44 mmol L^{-1} . Therefore it is uncertain if sorption would occur when soil solution NO_3^- concentrations are below this range, which is common. Within five differing vegetative communities at CHL that vary in elevation, mean annual soil solution NO_3^- concentrations range between 0.004 and 0.147 mg NO_3^- L^{-1} at a depth of 15 cm and 0.002 and 0.074 mg NO_3^- L^{-1} at depths >40cm (Knoepp et al. 2008). Since these values represent annual mean soil solution NO_3^- concentrations, NO_3^- sorption may occur within specific seasonal conditions where solution concentrations are elevated. Due to the spatial and temporal variability of NO_3^- leaching, further study must be employed to determine if the role of abiotic NO_3^- sorption on the retardation of NO_3^- leaching given the in situ NO_3^- concentrations in soil solution is significant.

The positive correlation between *b* and *a* suggests that horizons with a higher maximum capacity for sorption also have a longer transition from a threshold concentration, when the soil starts NO_3^- sorption, to the maximum NO_3^- sorption value. This relationship suggests that soils with a large capacity for anion sorption were more likely to have residual anion competition, influencing NO_3^- equilibration.

5.2 Soil Properties and Parameters

5.2.1 Sorption Isotherm Parameter *a*

Parameter *a* is positively correlated with Al_o, which has been found to be important in the retention of NO_3^- in a range of soils (Strahm & Harrison 2006). Al_o was also found to interact with other anions including total phosphorus (Igwe et al. 2010) and sulfate (SO_4^{2-}) (Kimsey et al. 2011, Alves & Lavorenti 2003). Ammonium oxalate extracts aluminosilicates, oxides, and hydroxides of Fe, Al and Mn (Schwertmann 1973, Mckeague & Day 1966, Mckeague et al. 1971, Fey & LeRoux 1977) suggesting that these forms have a higher potential than other extracted forms to be involved in NO_3^- retention. The Al_o has been shown to be a proxy for gibbsite ($Al(OH)_3$) concentrations (Jackson et al. 1986, Shaw 2001); a ubiquitous and potentially highly reactive amorphous Al-oxide (Essington 1994).

Mn_p and Mn_o represent organically bound and amorphous oxide forms of Mn, respectively (Jackson et al. 1986). Manganese oxides occur naturally in small amounts and are highly disordered and reactive (McKenzie 1980, Barlett & Ross 2005); however, it is unlikely they are participating in anion exchange because they require a pH < 2 to attain a net negative charge (Essington 2004). Therefore the correlations between the sorption parameter *a* and Mn are not likely to be directly related to NO_3^- sorption to Mn-oxides. They could be a result of Mn-

oxides sorbing to and potentially oxidizing monomeric Fe and Al (McKenzie 1980 & 1989, Feng et al. 2007), and/or a reflection of their spatial association with other secondary minerals (Table 2) (Barlett & Ross 2005, Negra et al. 2005). For instance, lithiophorite $\{(Al_2Li)(OH)_6Mn_2^{IV}Mn^{III}O_6\}$ takes on a gibbsite-like structure and has been identified in acidic Ultisols and Oxisols. Gibbsite nuclei in solution is necessary for lithiophorite formation (Vodyanitskii 2009). Therefore correlations between Mn_o and *a* may be a reflection of an association between Mn and gibbsite which the ammonium oxalate extraction also reflects.

Amorphous forms of Fe, represented by Fe_o (Jackson et al. 1986), have been shown to be active in NO_3^- (Kimsey et al. 2011) and sulfate sorption (Johnson &Todd 1983, Alves & Lavorenti 2003). Fe_o has been found to be a good representation of ferrihydrite, a poorly crystalline form of Fe-oxide, but not hematite and goethite, which are more stable forms of Fe-oxides (Parfitt & Childs 1988).

Fe_p, Al_p, Fe_d and Al_d were positively correlated with the sorption maximum ($p<0.05$). Fe_p has been found to represent ferrihydrite and Fe bound to organic matter (Parfitt and Childs 1988) while Al_p represents monomeric or simple hydroxyl polymers associated with soil organic matter (Parfitt and Childs 1988). The positive relationship between the organically bound fractions of metal oxides and the NO_3^- sorption maxima could be a result of C inhibiting the Fe and Al oxide crystallization (Schwertmann 1985) and/or an increase in reactive surfaces resulting from Fe and Al – organic matter interactions (Alves & Lavorenti 2003). This is also supported by the correlations between C and Fe_o, Al_o, Fe_p and Al_p (Table 2). Since the pyrophosphate and ammonium oxalate fractions of Fe and Al are also extracted in the dithionite extraction, we expect there to be correlations with the sorption parameters and Fe_d and Al_d.

5.2.2 Sorption Isotherm Parameters X_o and b

The positive relationship between X_o and b with percent soil C suggests that organic compounds, such as organic acids, are prohibiting the binding of NO_3^- to available sorption sites. Since the %C is positively associated with a wider sigmoidal curve width, the change in which NO_3^- transitions from the initiation of sorption toward reaching the sorption maximum is attenuated, less abrupt, in B- horizons that are higher in C. Organic matter has been found to cause NO_3^- exclusion from sorption (Black & Waring 1976, Johnson & Todd 1983, Toner et al. 1989, Wong et al. 1990) and C can be the primary cause of exclusion within the upper 120 cm of the soil mantle due to the negative charge of organic matter (Black & Waring 1976).

Al_o, Mn_o and were all positively related to X_o and b; this is contrary to the proposed mechanism for abiotic NO_3^- sorption in this study. We would expect that with increasing oxide contents would result in a decrease in X_o and b; displaying higher sorption at lower equilibrium concentration because a higher abundance of oxides would theoretically result in an increasing amount of available sorption sites. In this case, using parameters X_o and b does not assist in our understanding of how these soil properties relate to the NO_3^- sorption mechanism proposed in this study. Therefore the utility of parameters X_o and b is uncertain.

5.3 Multiple Regression Models

5.3.1 Sorption Isotherm Parameter *a*

Parameter *a* was predicted by three significant variables; Al_o, Mn_o/Mn_d, and depth (eq 4). Schwertmann et al. (1987) reported that a high Mn_o/Mn_d ratio (>0.9) in Finnish lake sediments indicated that Mn was present in a pure oxide form and not part of goethite. In this study the soils with Mn_o/Mn_d ratios >0.9 also exhibited the some of the highest sorption maximums and were

generally B2 horizons found near streams . Mn is soluble and mobile in the reduced form (McDaniel et al. 1992) and secondary Mn minerals have been shown to accumulate in saprolite underlying well drained Ultisols (Calvert et al. 1980). The increase of Mn_o in Bt2 or Bw2 horizons and near streams environments may be an indication of transport and accumulation patterns of translocated Mn that is not bound to organic matter and may be in a more available form to interact with Fe and Al. Although it is unlikely that Mn-oxides are directly related to NO_3^- sorption due to their generally low points of zero net charge (Essington 2004), the precipitation of Mn may be indicative of other secondary minerals that can sorb NO_3^- yet were not able to be detected through selective dissolution analysis.

Depth serves as a very non-specific variable that may be capturing a chemical property that we did not measure specifically in this study. Since depth was not significantly related to Al_o ($r=0.21$, $p=0.12$), this may serve as a general index a combination or the interaction of multiple biogeochemical soil properties that are favorable for NO_3^- sorption.

5.3.2 Sorption Isotherm Parameter *b*

The model for parameter *b* included the %C, which explained ~ 68% of the variance. Soil horizons with an elevated present carbon also exhibited a larger the transition between sorption initiation and the maximum sorption capacity. This is most likely due to organic matter preferentially binding to positive exchange sites or covering up mineral surfaces (Black and Waring 1976).

5.3.3 Sorption Isotherm Parameter X_o

The multiple regression model for parameter X_o had a low r^2 value despite the use of three significant predictive variables. Additionally, the correlation coefficient between X_o and %C was positive however the regression coefficient for %C in the model is negative. As a result, we have chosen not to pursue X_o in the as it does not serve as an informative descriptive variable for abiotic NO_3^- sorption within the soils used in this study.

5.3.4 Model Uncertainty

Although there is value in exploring these models and interpreting significant predictors of each parameter response variable, there was a lack of a strong goodness of fit for parameters X_o and a. The models appear to be underspecified, making them biased estimates. This means that essential explanatory variables were not measured in this study or that the measurements taken were not accurate enough to explain the true cause of variation in NO_3^- sorption. Variation in soil chemical properties does not appear to be able to predict variation in parameters values at the scale of these observations. The indices derived from selective dissolution techniques may be too coarse to determine mineralogical differences driving the variation in sorption isotherm parameters when comparing fractions at a local scale. Using selective dissolution techniques for comparing soils with highly contrasting mineralogy (i.e., different soil orders) in spatially isolated ecosystems has been shown to explain more variation sorption (Strahm & Harrison 2007). Additionally, the range of pH was limited to the natural variation that existed within the study watersheds and was not adjusted in the laboratory prior to the implementation of batch equilibrium techniques. Although it is theoretically well understood that increases in acidity tend to result in higher anion sorption, given the proper mineralogy, the field range of pH used in this study may not have been large enough to account for variation in NO_3^- sorption despite the

theoretical understanding of the role of H^+ as a potential determining ion for variable charge soil minerals.

5.4 Watershed Variability

Disturbed watersheds had higher variability in parameters X_o and b as shown by the width of the upper and lower quartiles and the larger distribution of data (Figure 5). The increased variability in X_o and b in the disturbed watersheds may be related to higher variability in soil solution chemistry. There is no increase in the variability of C or pH in disturbed watersheds compared to reference (Table 3). This variability in the disturbed watersheds may be dependent upon the season and the moisture content of the soil as soil solution varies depending upon many biological processes and the concentrations of dissolved soil constituents in the solution phase. Our sampling period took place after a high intensity precipitation event. The ionic composition at the soil solution and soil colloidal interface may have been different than equilibrium concentrations prior to the precipitation event. The increased variability of the isotherm curves in disturbed watersheds (Figure 5) could be an indication of higher spatial variability in soil solution ionic strength and solute composition within disturbed watersheds. This suggests that land use history may play a larger role influencing NO_3^- sorption behavior than other edaphic factors within any particular system.

The data and geologic history suggest mineralogical differences between the upper and lower elevation watersheds. The median percent Al_p, Fe_p, Al_o and Fe_o were higher in the DH watershed (Table 3); the 25% quartile did not overlap with the 75% quartiles of the DL and RL watersheds and Al_o was positively correlated with elevation ($r=0.47$, $p<0.00$). Maximum sorption capacity also shows a larger distribution with the larger values in the high elevation disturbed

watersheds, relating these differences in geology back to NO_3^- sorption. This suggests that there are more amorphous and organically bound oxides within upper watersheds. Watersheds on the southern side of the Shope Fork Fault at CHL, part of the Coleman River Formation, have been found to have less biotite and plagioclase than RL, which contains part of the Otto formation. Coleman River Formation parent materials were found to form more gibbsite and much less vermiculite and kaolinite than those found in RL (Price et al. 2005).

Fe_o/Fe_d and Al_o/Al_d can be indicators of the degree of soil weathering (Bera et al. 2004). Ratios below 1 indicate that the soil is an advanced stage of aging and has high crystallinity. As soils progress in age, amorphous oxides tend to crystalize. More crystalized forms of oxides have less surface area and potential surface charge than amorphous forms. The median Fe_o/Fe_d ratios for horizons in the high elevation watersheds were generally higher than low elevation watersheds (Table 3). The median Al_o/Al_d ratio values for the watersheds followed the same pattern but were less distinct due to the overlap in 25 and 75 % quartiles between watersheds. Higher elevation soils, comprised primarily of Inceptisols, are less developed soils relative to low elevation soils and have a higher abundance of oxalate and pyrophosphate extractable Fe and Al. Lower elevation soils are showing signs of progressing toward crystalline oxide forms and have a higher abundance of Ultisols. In conjunction with the results from the isotherm analysis, it appears that within the CHL basin, less developed soils with elevated Al_o have a higher capacity for NO_3^- and are associated with Al-humus and Fe-humus compounds.

Results from this study suggest that there may be a potential for NO_3^- sorption deeper in the soil profile. Boul and Weed (1991) observed a decrease in hydrologic conductivity at the BC/Cr interface in soils within the Piedmont and Mountain Provinces of North Carolina. This was due to the presence of translocated clays that created thick cutans. Oxide accumulation

within these regions of the soil profile can serve as anion exchange sites. Furthermore, Calvert et al. 1980 studied the weathering of a profile that was developed on granitic gneiss in the North Carolina Piedmont and found that feldspar weathering at the saprolite and rock interface produced gibbsite and other amorphous aluminosilicates. McVay et al. (2004) found that the anion exchange capacity in saprolite within Northern Georgia Piemont soils was positively related to Fe oxides. Although the anion exchange capacity of the topsoil was two times greater than the underlying saprolite, the volume of the saprolite zone relative to the solum allows for saprolite to be a potential ecosystem NO_3^- sink. However more work needs to be done to understand the potential role of the transitional zone between the soil mantel and the saprolite for NO_3^- retention. Lower elevation watersheds with more developed soils may exhibit a larger, more weathered saprolite zone that may serve as temporary NO_3^- sink. This information can be beneficial in understanding stream water NO_3^- dynamics.

6. CONCLUSIONS

The S-shape of the isotherm suggests that NO_3^- is not immediately sorbed to soil colloidal surfaces and a threshold concentration must be overcome in order for NO_3^- to be a competitor for sorption sites. The higher affinity of NO_3^- for soil solution than for the soil colloidal surface at low concentrations could be a result of organic matter binding to positively changed sites at the soil solution interface, organic matter covering the mineral surface, or the low soil solution ionic strength at the time in which the soils were sampled. As a result, NO_3^- sorption maybe a spatially and temporally variable mechanism; for instance during periods when ambient soil solution ionic strength is lower.

The presence of C and competing anions in the upper B horizons also appears to be decreasing any potential for NO_3^- to sorb. This study suggests that soil C inhibits NO_3^- sorption with B horizons in the upper soil mantel. However, lower B horizons appear to have a higher capacity for sorption (Figure 4). NO_3^- sorption may increase with vertical distance from the soil-atmosphere interface, where biologically mediated processes and cycling are less pervasive. The highest potential for sorption maybe an intermediate zone between where there is a significant decrease in biologically cycled C, phosphate and sulfate yet there is enough mineral weathering to provide the mineralogical structures that can support positively charged surfaces.

Landscape variation in Al extracted by ammonium oxalate relates to the variation in the sorption maximum for B horizons suggesting that this fraction may represent an amorphous Al-oxide that hosts positive exchange sites within this system. Still other oxide fractions such as Fe_o, Al_p and Fe_p are positively related to the sorption maxima and may participate in NO_3^- sorption. Within the four watersheds examined in this study, deeper B horizons within the higher elevation watersheds appear to have the strongest potential for NO_3^- sorption due to mineralogical differences from low elevation watersheds.

In order to determine the applicability of this work to stream NO_3^- concentrations and fluxes, further research must be employed in order to fully understand the relevance of this mechanism within the ecosystem. The atypical shape of the isotherms resulting from this study suggests a possible temporal sensitivity of NO_3^- sorption. The data from this study also suggests further investigation of deeper soil zones that may behave differently than the upper soil mantle.

7. SUMMARY

Anthropogenic reactive N has increased in ecosystems due to various land management practices and as a non-point source pollutant. As N is a limiting nutrient in most ecosystems, this has had both positive and adverse effects on ecosystem vitality and services. Increases in N generally produce higher biomass but have also been shown to increase groundwater and runoff N thereby decreasing water quality. Source of reactive N have increased through the combustion of fossil fuels; leading to both dry and wet atmospheric N deposition. Understanding the effects of this atmospherically derived N on forested systems is important for determining acute and long-term impacts on ecosystem N dynamics and water quality.

Soils can serve as a biotic and abiotic sink for N. NO_3^- is highly mobile and is subject to leaching to ground and surface waters. Abiotic NO_3^- retention can temporarily retard NO_3^-, increasing its residence time in the system and by extension its biological availability. Determining if abiotic NO_3^- retention is a significant mechanism in NO_3^- retention may aid our understanding of NO_3^- dynamics and annual fluctuations in stream water N.

Forest mountain watershed soils are complex and highly variable, with many different physiographic and geologic factors influencing their formation. Understanding how biogeochemical processes differ spatially and temporally with watershed soils can be a crucial component for predicting headwater stream inorganic and organic exports. At the Coweeta Hydrologic Laboratory (CHL) we evaluated NO_3^- sorption as a mechanism for abiotic NO_3^- retention. Samples were taken from four watersheds; high and low elevation disturbed and reference watersheds. NO_3^- sorption was determined using batch equilibration techniques on A,

B and B2 soil horizons from 42 sample plots. Soil chemistry data (e.g., selective dissolution analyses, %C, S_{CaPO4}, pH) was used to explain differences in the observed sorptive behaviors.

NO_3^- sorption isotherms exhibited an S-shape curve for B horizons, indicating that NO_3^- has a higher affinity for soil solution than the soil colloidal surfaces at low equilibrium solution concentrations. A-horizons exhibited minimal sorption with no distinct pattern with increasing equilibrium concentrations. A three parameter, sigmoid, logistic model was fit to the sorption data from each B horizon and sorption isotherm parameter values (a, X_o, and b) were derived. Parameter a, the sorptive maximum, was most strongly correlated to Al_o and Mn_o, suggesting the role of amorphous forms of Al and Mn oxides in the abundance and availability of positively charged sorption sites. Parameter b, the width of the sigmoid curve, was best predicted by the % C, emphasizing the role of C in coating positively charged exchange sites that could potentially host NO_3^-or that soil organic matter may cover mineral surfaces decreasing the overall charge. Parameter $X_{o,}$ the inflection point of the curve, did not assist in our understanding of how soil chemical properties relate to the NO_3^- sorption mechanism proposed in this study.

Disturbed high and low elevation watersheds exhibited a larger amount of variability in parameter values which could indicate a larger variation in soil or soil solution chemistry than reference watersheds. Higher elevation watersheds had higher median values for Al_o and Fe_o than low elevation watersheds. This suggests a difference in weathering rates, which is likely due to differences in climate and parent material (Price et al. 2005). Additionally, higher elevation watersheds had higher Fe_o/Fe_d ratios, indicating that the soils at higher elevations are less developed relative to low elevation soils and have more free amorphous Fe and Al oxides that have not been reprecipitated or crystalized.

Although NO_3^- sorption does occur within these soils, an equilibrium NO_3^- concentration threshold must be overcome in order to initiate sorption. Soil solution NO_3^- concentrations attained from lysimeters in previous studies at CHL (Knoepp et al. 2008) are not high enough to initiate NO_3^- sorption based upon the isotherms used in this study. However more spatially and temporally sensitive work must be employed to thoroughly understand the relevance of NO_3^- sorption in this system under the current environmental conditions. C appears to be decreasing the potential for NO_3^- to sorb. Lower B horizons appear to have a higher capacity for sorption (Figure 4); NO_3^- sorption appears to increase with vertical distance from the soil-atmosphere interface, where biologically mediated processes and cycling are less pervasive and where mineral weathering and oxide accumulations exist. Further study may benefit in understanding how BC, Cr (saprolite) and other deeper horizons may play a role in NO_3^- sorption.

8. LITERATURE CITED

Aber JD (1992) Nitrogen cycling and nitrogen saturation in temperate forest ecosystems. Trends in Ecology & Evolution 7(7): 220-224

Alves ME, Lavorenti A (2004) Sulfate adsorption and its relationships with properties of representative soils of the Sao Paulo State, Brazil. Geoderma 118(1-2): 89-99

Bartlett RJ, and Ross DS (2005) Redox processes in soils. In D.L. Sparks and A. Tabatabai (ed.) Chemical processes in soils. SSSA Book Series No. 8. SSSA, Madison, WI.

Bera R, Seal A, Banerjee M, Dolui A K (2005) Nature and profile distribution of iron and aluminum in relation to pedogenic processes in some soils developed under tropical environment in India. Earth and Environmental Science 47(2): 241-245

Black AS, Waring SA (1976) Nitrate leaching and adsorption in a Krasnozem from Redland Bay QLD.2. Soil factors influencing adsorption. Australian Journal of Soil Research 14(2): 181-188

Bolan NS, Naidu R, Syers JK, Tillman RW (1999) Surface charge and solute interactions in soils. In: Advances in Agronomy, Vol 67. Advances in Agronomy. Academic Press Inc, San Diego. p 87-140

Bonito GM, Coleman DC, Haines BL, Cabrera ML (2003) Can nitrogen budgets explain differences in soil nitrogen mineralization rates of forest stands along an elevation gradient? Forest Ecology and Management 176(1-3): 563-574

Boul SW, Weed SB (1991) Saprolite-soil transformations in the Piedmont and mountains of North Carolina. Geoderma 51: 15-28

Bouwman AF, Van Vuuren DP, Derwent RG, Posch M (2002) A global analysis of acidification and eutrophication of terrestrial ecosystems. Water Air and Soil Pollution 141(1-4): 349-382

Bowden RD, Melillo JM, Steudler PA, Aber JD (1991) Effects of nitrogen additions on annual nitrous-oxide fluxes from temperate forest soils in the northeastern Unites-Sates. Journal of Geophysical Research-Atmospheres 96(D5): 9321-9328

Brooks PD, Williams MW, Schmidt SK (1996) Microbial activity under alpine snowpacks, Niwot Ridge, Colorado. Biogeochemistry 32(2): 93-113

Burt TP, Matchett LS, Goulding KWT, Webster CP, Haycock NE (1999) Denitrification in riparian buffer zones: the role of floodplain hydrology. Hydrological Processes 13(10): 1451-1463

Burt TP, Pinay G (2005) Linking hydrology and biogeochemistry in complex landscapes. Progress in Physical Geography 29(3): 297-316

Cahn MD, Bouldin DR, Cravo MS (1992) Nitrate sorption in the profile of an acid soil. Plant and Soil 143(2): 179-183

Calvert CS, Buol SW, and Weed SB (1980) Mineralogical characteristics and transformations of a rock-saprolite-soil profile in the North Carolina Piedmont. I. Profile morphology, chemical composition, and minerology. Soil Sci. Soc. Am. J. 44:1096-1103.

Calvert CS, Buol SW, and Weed SB (1980) Mineralogical characteristics and transformations of a rock-saprolite-soil profile in the North Carolina Piedmont. II. Feldspar alteration products - Their transformation through the profile. Soil Sci. Soc. Am. J. 44:1104-1112.

Campbell JL, Hornbeck JW, Mitchell MJ, Adams MB, Castro MS, Driscoll CT, Kahl JS, Kochenderfer JN, Likens GE, Lynch JA, Murdoch PS, Nelson SJ, Shanley JB (2004) Input-output budgets of inorganic nitrogen for 24 forest watersheds in the northeastern United States: A review. Water Air and Soil Pollution 151(1-4): 373-396

Colman BP, Fierer N, Schimel JP (2007) Abiotic nitrate incorporation in soil: is it real? Biogeochemistry 84(2): 161-169

Dail DB, Davidson EA, Chorover J (2001) Rapid abiotic transformation of nitrate in an acid forest soil. Biogeochemistry 54(2): 131-146

Davidson EA, Chorover J, Dail DB (2003) A mechanism of abiotic immobilization of nitrate in forest ecosystems: the ferrous wheel hypothesis. Global Change Biology 9(2): 228-236

Davidson EA, Dail DB, Chorover J (2008) Iron interference in the quantification of nitrate in soil extracts and its effect on hypothesized abiotic immobilization of nitrate. Biogeochemistry 90(1): 65-73

Day FP, Philips DL, Monk CD (1988) Forest communities and patterns, in Forest Hydrology and Ecology at Coweeta, edited by W. T. Swank and D. A. Crossley Jr., pp. 141–149, Springer, New York.

Dittman JA, Driscoll CT, Groffman PM, Fahey TJ (2007) Dynamics of nitrogen and dissolved organic carbon at the Hubbard Brook Experimental Forest. Ecology 88(5): 1153-1166

Driscoll C, Whitall D, Aber J, Boyer E, Castro M, Cronan C, Goodale C, Groffman P, Hopkinson C, Lambert K, Lawrence G, Ollinger S (2003) Nitrogen pollution: Sources and consequences in the US northeast. Environment 45(7): 8-+

Eick MJ, Brady WD, Lynch CK (1999) Charge properties and nitrate adsorption of some acid Southeastern soils. Journal of Environmental Quality 28(1): 138-144

Essington ME (2004) Soil and water chemistry: an integrative approach. CRC Press LLC, 2000 N.W. Corporate Blvd., Boca Raton, Florida

Feng XH, Zhai LM, Tan WF, Liu F, He JZ (2007) Adsorption and redox reactions of heavy metals on synthesized Mn oxide minerals. Environmental Pollution 147(2):366-373

Fox R L, Olsen R A and Rhoades H F (1964) Evaluating the sulfur status of soils by plant and soil tests. Soil Sci. Soc. Am. Proc. 28: 243–246.

Goodale CL, Aber JD, Vitousek PM (2003) An unexpected nitrate decline in New Hampshire streams. Ecosystems 6(1): 75-86

Grant PG, Lemke SL, Dwyer MR, Phillips TD (1998) Modified Langmuir equation for S-shaped and multisite isotherm. Langmuir 14(15): 4292-4299

Green PA, Vorosmarty CJ, Meybeck M, Galloway JN, Peterson BJ, Boyer EW (2004) Pre-industrial and contemporary fluxes of nitrogen through rivers: a global assessment based on typology. Biogeochemistry 68(1): 71-105

Gundersen P, Callesen I, de Vries W (1998) Nitrate leaching in forest ecosystems is related to forest floor C/N ratios. Environmental Pollution 102: 403-407

Gustafsson JP, Jacks G (1993) Sulphur status in some Swedish podzols as influenced by acidic deposition and extractable organic carbon. Environmental Pollution 81(2):185-191

Hatcher, R.D. (1980) Geologic map of Coweeta Hydrologic Laboratory, Prentiss Quadrangle, North Carolina, scale 1:14,400. State of North Carolina, Department of Natural Resources and Community Development, in Cooperation with the Tennessee Valley Authority.

Hatcher R.D (1988) Bedrock geology and regional geologic setting of Coweeta Hydrologic Laboratory in the Eastern Blue Ridge. In W.T. Swank and D.A. Crossley, Jr., Eds., Forest Hydrology and Ecology at Coweeta. Springer-Verlag, New York: 81-92

Hinz C (2001) Description of sorption data with isotherm equations. Geoderma 99(3-4): 225-243

Hultberg H, Dise NB, Wright RF, Andersson I, Nystrom U (1994) Nitrogen saturation induced during winter by experimental NH4NO3 addition to a forested catchment. Environmental Pollution 84(2): 145-147

Igwe CA, Zarei M, Stahr K (2010) Fe and Al oxides distribution in some ultisols and inceptisols of southeastern Nigeria in relation to soil total phosphorus. Environmental Earth Sciences 60(5): 1103-1111

Johnson DW, Cheng W, Burke IC (2000a) Biotic and abiotic nitrogen retention in a variety of forest soils. Soil Science Society of America Journal 64(4): 1503-1514

Johnson DW, Cheng W, Burke IC (2000b) Biotic and abiotic nitrogen retention in a variety of forest soils. Soil Science Society of America Journal 64(4): 1503-1514

Johnson DW, Cheng W, Burke IC (2000c) Biotic and abiotic nitrogen retention in a variety of forest soils. Soil Science Society of America Journal 64(4): 1503-1514

Johnson DW, Todd DE (1983) Relationships amoung iron, aluminum, carbon, and sulfate in a variety of forest soils. Soil Science Society of America Journal 47(4): 792-800

Kimsey MJ, Garrison-Johnston MT, Johnson L (2011) Characterization of Volcanic Ash-Influenced Forest Soils across a Geoclimatic Sequence. Soil Science Society of America Journal 75(1): 267-279

Knoepp JD, Clinton BD (2009) Riparian zones in southern Appalachian headwater catchments: Carbon and nitrogen responses to forest cutting. Forest Ecology and Management 258(10): 2282-2293

Knoepp JD, Swank WT (1998) Rates of nitrogen mineralization across an elevation and vegetation gradient in the southern Appalachians. Plant and Soil 204(2): 235-241

Knoepp JD, Swank WT (2002) Using soil temperature and moisture to predict forest soil nitrogen mineralization. Biology and Fertility of Soils 36(3): 177-182

Knoepp JD, Vose JM (2007) Regulation of nitrogen mineralization and nitrification in Southern Appalachian ecosystems: Separating the relative importance of biotic vs. abiotic controls. Pedobiologia 51(2): 89-97

Knoepp JD, Vose JM, Swank WT (2008) Nitrogen deposition and cycling across an elevation and vegetation gradient in southern Appalachian forests. International Journal of Environmental Studies 65(3): 389-408

Magill AH, Aber JD, Hendricks JJ, Bowden RD, Melillo JM, Steudler PA (1997) Biogeochemical response of forest ecosystems to simulated chronic nitrogen deposition. Ecological Applications 7(2): 402-415

McDaniel PA, Bathke GR, Buol SW, Cassel DK, Falen AL (1992) Secondary Manganese Iron ratios as Pedochemical Indicators of Field-Scale Throughflow Water Movement. Soil Science Society of America Journal 56(4): 1211-1217

McKeague JA, Day JH (1966) Dithionite-and oxalate- extractable Fe and Al as aids in differentiating various classes of soils. Canadian Journal of Soil Science 46(1): 13-22

McKeague JA, Brydon JE, Miles NM (1971) Differentiation of forms of extractable iron and aluminum in soils. Soil Science Society of America Journal 35(1): 33-38
McKenzie RM (1980) The adsorption of lead and other heavy metals on oxides of manganese and iron. Aust. J. Soil Res. 18:61–73.

McKenzie RM (1989) Manganese oxides and hydroxides. *In* J.B. Dixon and S.B. Weed (ed.) Minerals in soil environments. SSSA, Madison, WI. 439–465

McVay KA, Radcliffe DE, West LT, Cabrera ML (2004) Anion exchange in saprolite. Vadose Zone Journal 3(2): 668-675

Meyer PS, Yung JW, Ausubel JH (1999) A primer on logistic growth and substitution - The mathematics of the Loglet Lab software. Technological Forecasting and Social Change 61(3): 247-271

Nadelhoffer KJ, Aber JD, Melillo JM (1984) Seasonal patterns of ammonium and nitrate uptake in 9 temperate forest ecosystems. Plant and Soil 80(3): 321-335

Negra C, Ross DS, Lanzirotti A (2005a) Oxidizing behavior of soil manganese: Interactions among abundance, oxidation state, and pH. Soil Science Society of America Journal 69(1): 87-95

Ohrui K, Mitchell MJ, Bischoff JM (1999) Effect of landscape position on N mineralization and nitrification in a forested watershed in the Adirondack Mountains of New York. Canadian Journal of Forest Research-Revue Canadienne De Recherche Forestiere 29(4): 497-508

Palmer SM, Driscoll CT, Johnson CE (2004) Long-term trends in soil solution and stream water chemistry at the Hubbard Brook Experimental Forest: relationship with landscape position. Biogeochemistry 68(1): 51-70

Parfitt RL, Childs CW (1988) Estimation of forms of Fe and Al- A review, and analysis of contrasting soils by dissolution and Mossbauer methods. Australian Journal of Soil Research 26(1): 121-144

Parfitt RL, Fraser AR, Russell JD, Farmer VC (1977) Adsorption on hydrous oxides.2. Oxalate, benzoate and phosphate on gibbsite. Journal of Soil Science 28(1): 40-47

Price JR, Patino LC, Velbel MA (2005a) Geochemical mass balances and weathering rates in forested watersheds of the Southern Blue Ridge: Solving more equations in more unknowns through incorporation of rare earth elements. Geochimica Et Cosmochimica Acta 69(10): A755-A755

Price JR, Velbel MA (2003) Chemical weathering indices applied to weathering profiles developed on heterogeneous felsic metamorphic parent rocks. Chemical Geology 202(3-4): 397-416

Price JR, Velbel MA, Patino LC (2005b) Rates and time scales of clay-mineral formation by weathering in saprolitic regoliths of the southern Appalachians from geochemical mass balance. Geological Society of America Bulletin 117(5-6): 783-794

Qualls RG (2000) Comparison of the behavior of soluble organic and inorganic nutrients in forest soils. Forest Ecology and Management 138(1-3): 29-50

Qualls RG, Haines BL, Swank WT, Tyler SW (2002) Retention of soluble organic nutrients by a forested ecosystem. Biogeochemistry 61(2): 135-171

Rice TJ, Weed SB, Buol SW (1985b) Soil saprollite profiles derived from mafic rocks in the North Carolina Piedmont. 2. Association of free iron-oxides with soils and clays. Soil Science Society of America Journal 49(1): 178-186

Ross DS, Wemple BC, Jamison AE, Fredriksen G, Shanley JB, Lawrence GB, Bailey SW, Campbell JL (2009) A Cross-Site Comparison of Factors Influencing Soil Nitrification Rates in Northeastern USA Forested Watersheds. Ecosystems 12(1): 158-178

Schiff SL, Devito KJ, Elgood RJ, McCrindle PM, Spoelstra J, Dillon P (2002) Two adjacent forested catchments: Dramatically different NO3- export. Water Resources Research 38(12): 13

Schoeneberger PJ, Amoozegar A, Buol SW (1995) Physical Property variation of a soil and saprolite continuum at 3 Geomorphic positions. Soil Science Society of America Journal 59(5): 1389-1397

Schmidt BH, Matzner E (2009) Abiotic reaction of nitrite with dissolved organic carbon? Testing the Ferrous Wheel Hypothesis. Biogeochemistry 93: 291-296

Schwertmann U, Carlson L, Murad E (1987) Properties of Iron-Oxides in 2 Finnish lakes in relation to the environment of the formation. Clays and Clay Minerals 35(4): 297-304

Schwertmann, U (1973) Use of oxalate for Fe extraction from soils. Can. J. Soil Sci. 53: 244–246.

Shaw JN (2001) Iron and aluminum oxide characterization for weathered Alabama Ultisols. Communications in Soil Science and Plant Analysis 32(1-2): 49-64

Soil Survey Staff, Natural Resource Conservation Service, USDA, Web Soil Survey. Available online at http://websoilsurvey.nrcs.usda.gov/. Accessed [October/10/2010].

Strahm BD, Harrison RB (2006) Nitrate sorption in a variable-charge forest soil of the Pacific Northwest. Soil Science 171(4): 313-321

Strahm BD, Harrison RB (2007) Mineral and organic matter controls on the sorption of macronutrient anions in variable-charge soils. Soil Science Society of America Journal 71(6): 1926-1933

Strahm BD, Harrison RB (2008) Controls on the Sorption, Desorption, and Mineralization of Low-Molecular-Weight Organic Acids in Variable-Charge Soils. Soil Science Society of America Journal 72(6): 1653-1664

Swank WT, Vose JM (1997) Long-term nitrogen dynamics of Coweeta forested watersheds in the southeastern United States of America. Global Biogeochemical Cycles 11(4): 657-671

Tani M, Okuten T, Koike M, Kuramochi K, Kondo R (2004) Nitrate adsorption in some andisols developed under different moisture conditions. Soil Science and Plant Nutrition 50(3): 439-446

Toner CV, Sparks DL, Carski TH (1989) Anion-exchange chemistry of middle atlantic soils-charge properties and nitrate retention kinetics. Soil Science Society of America Journal 53(4): 1061-1067

Velbel MA (1992) Geochemical mass balance and weathering rates in forested watersheds of the southern Blue Ridge.3. Cation budgets and the weathering rate of amphibole. American Journal of Science 292(1): 58-78

Velbel MA, Price JR (2007) Solute geochemical mass-balances and mineral weathering rates in small watersheds: Methodology, recent advances, and future directions. Applied Geochemistry 22(8): 1682-1700

Vitousek PM, Aber JD, Howarth RW, Likens GE, Matson PA, Schindler DW, Schlesinger WH, Tilman GD (1997) Human alteration of the global nitrogen cycle: Sources and consequences. Ecological Applications 7(3): 737-750

Vitousek PM, Dantonio CM, Loope LL, Westbrooks R (1996) Biological invasions as global environmental change. American Scientist 84(5): 468-478

Wong MTF, Hughes R, Rowell DL (1990) Retarded leaching of nitrate in acid soils from the tropics- measurement of the effective anion-exchange capacity. Journal of Soil Science 41(4): 655-663

Xu RK, Li JY, Ji GL (2005a) Effect of low molecular weight organic anions on adsorption of aluminum by variable charge soils. Water Air and Soil Pollution 168(1-4): 249-265

Xu RK, Yang ML, Wang QS, Ji GL (2005b) Effect of low molecular weight organic anions on the adsorption of NO3- by variable charge soils. Soil Science and Plant Nutrition 51(5): 663-666

Yeakley JA, Swank WT, Swift LW, Hornberger GM, Shugart HH (1998) Soil moisture gradients and controls on a southern Appalachian hillslope from drought through recharge. Hydrology and Earth System Sciences 2(1): 41-49

Vodyanitskii Yu (2009) Mineralogy and geochemistry of manganese: A review of publications. Eurasian Soil Science 42(10): 1170-117

9. APPENDIX

9.1 Figures and Tables Captions

Figure 1. (a) Geologic map of the southern Appalachian orogen from Price et al. 2005 (b) Coweeta Hydrologic Laboratory basin and experimental watersheds from Swank & Vose 1997.

Figure 2. Study watersheds of the Coweeta Hydrologic Laboraoty, including high elevation watersheds (a) 36 (reference) and 37 (disturbed); low elevation watersheds 2 (reference) and 7 (disturbed). Sample point (●) identification is represented by the adjacent letter.

Figure 3. The amount of NO_3^- sorbed [q (mmol kg of $soil^{-1}$)] relative equilibrium solution NO_3^- concentrations [C_{eq} (mmol NO_3^-)]. Each panel represents A-horizon soils stratified by elevation (high,low) and disturbance regime (reference, disturbed)

Figure 4. The amount of NO_3^- sorbed [q (mmol kg of $soil^{-1}$)] relative equilibrium solution NO_3^- concentrations [C_{eq} (mmol NO_3^-)]. Curves represent the best fit of a three parameter, sigmoid, logarithmic model. Each panel represents B-horizon soils stratified by elevation (high,low) and disturbance regime (reference, disturbed)

Figure 5. Box plots for sorption isotherm parameters a, X_o and b for study watersheds stratified by elevation [high (H), low (L)] and disturbance regime [reference (R), disturbed (D)]. Sample sizes for the analysis are: RL=10, DL=19, RH=15, and DH=14

Table 1. Spearman's correlations between sorption isotherm parameters a, X_o and b and soil chemical properties. Asterisks indicate significance as * p = 0.1-0.05, ** $p < 0.05$.

Table 2. Spearman's correlation matrix among soil chemical properties. Asterisks indicate significance as * p = 0.1-0.05, ** $p < 0.05$.

Table 3. Median values for soil chemical properties for study watersheds stratified by elevation [high (H), low (L)] and disturbance regime [reference (R), disturbed (D)]. Sample sizes for the analysis are: RL=10, DL=19, RH=15, and DH=14. Lower (25%) and upper (75%) quartile ranges are listed in parentheses.

Table 4. Soil chemical properties grouped by elevation and soil series (a) high elevation watersheds (b) low elevation watersheds. Abbreviated symbols represent the Cullasaja-Tuckasegee (Cu), Ednyville (Ed), Cleavland (Rk), Plott (Pw), Chandler (Cd) and Fannin (Fa) soil series.

Table5. Soil chemical properties aggregate by horizon and slope position. Selective dissolution fractions are represented as a %. Shoulder (S), backslope (B), footslope (F), and toeslope (T).

Table 6. Soil chemical properties aggregate by horizon and local landform elements (Schmidt & Hewitt 2004). Selective dissolution fractions are represented as a %. Planar slope (ss), hollow (sv), spur (sx), hollow foot (vv), shoulder slope (xs), and nose (xx).

9.1.1 Figure 1

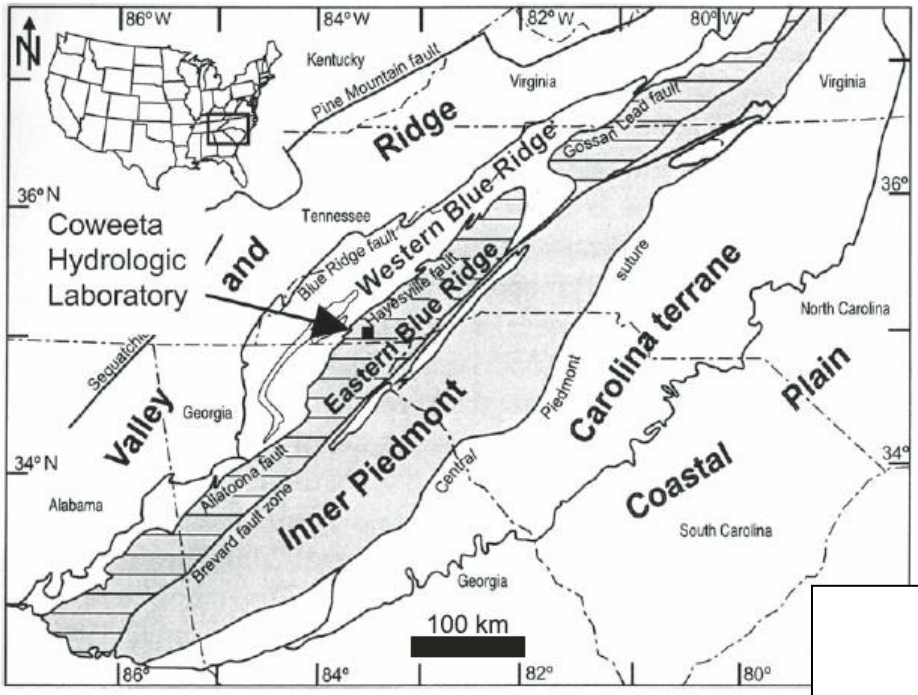

a

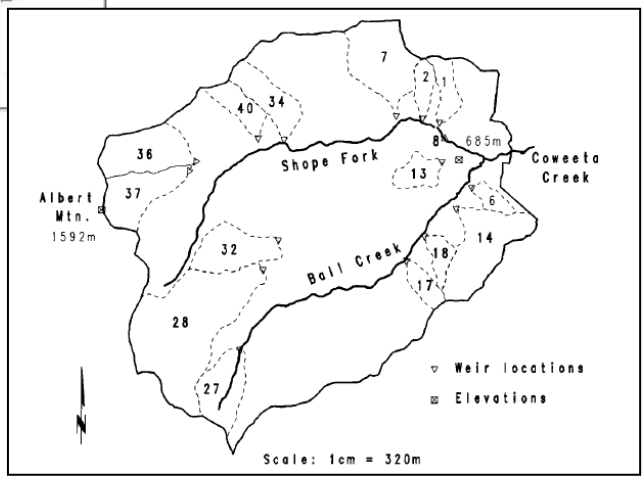

b

9.1.2 Figure 2

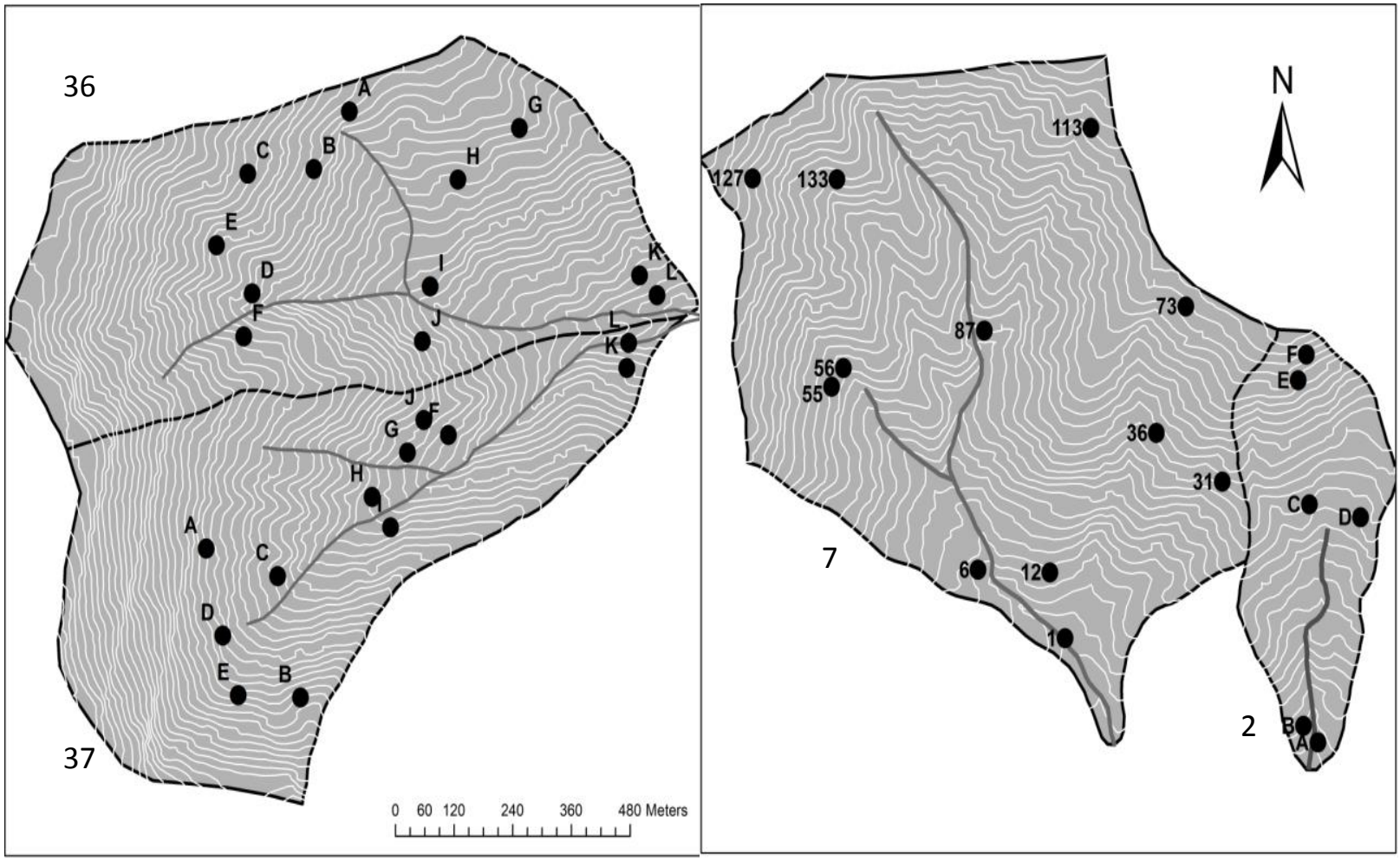
36
A
G
C
B
H
E
D
I
K
L
F
J
L
K
J
F
G
H
A
C
D
E
B
37
0 60 120 240 360 480 Meters
N
113
127
133
73
87
F
E
56
55
36
31
C
D
7
6
12
1
2
B
A

9.1.3 Figure 3

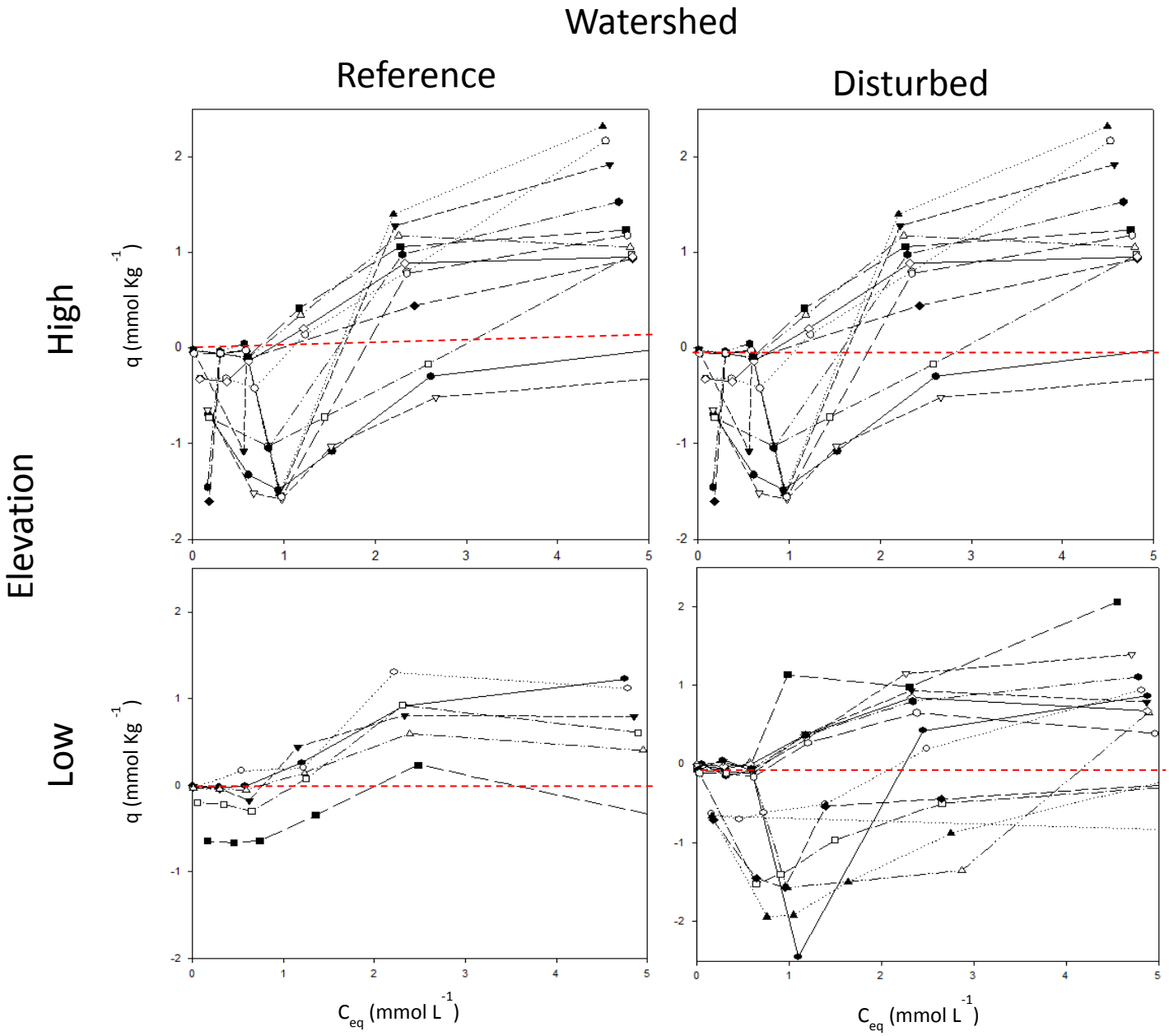
Watershed
Reference
Disturbed
Elevation
High
Low
q (mmol Kg-1)
Ceq (mmol L-1)

9.1.4 Figure 4

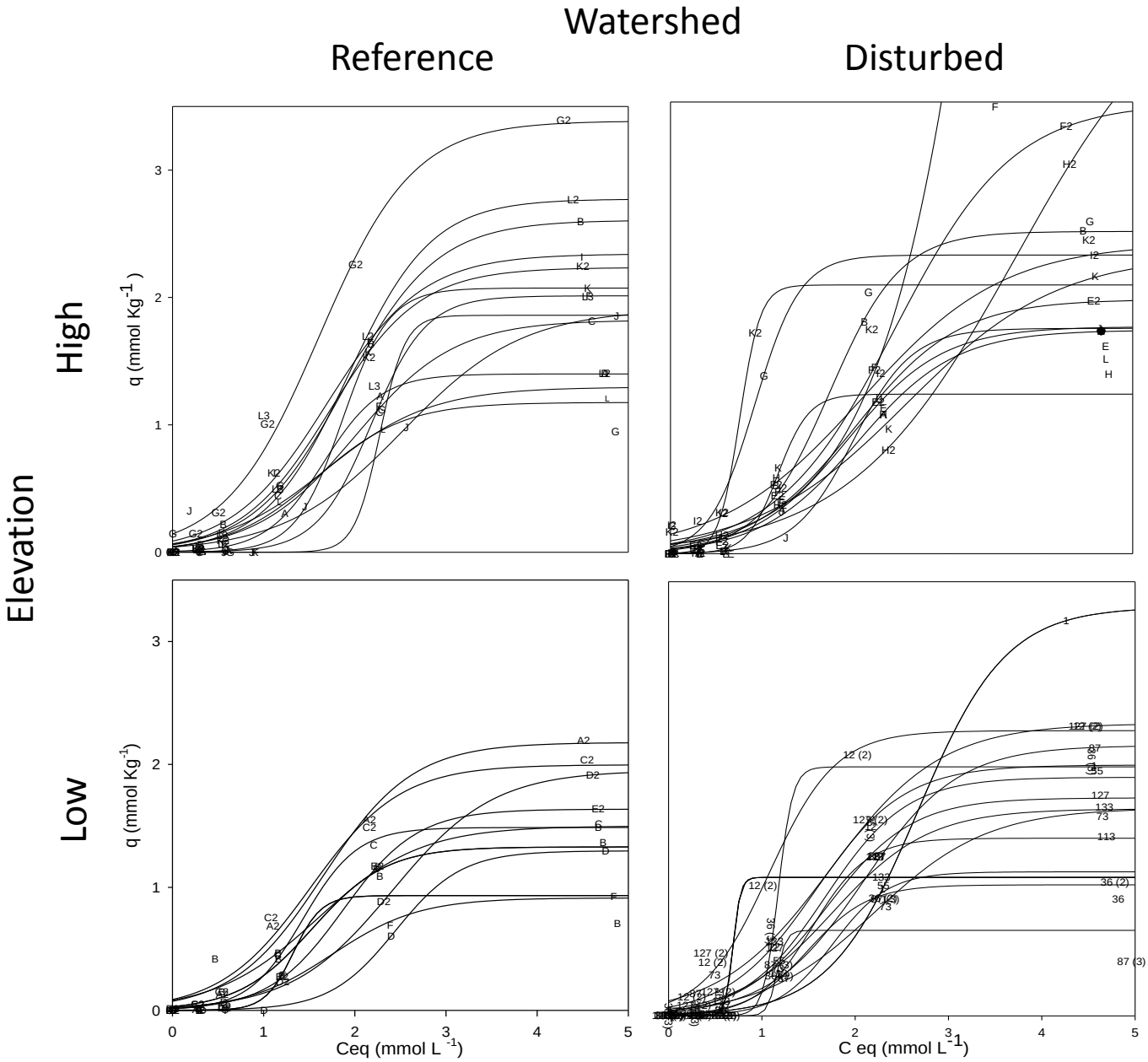
Watershed
Reference
Disturbed
Elevation
High
Low
q (mmol Kg-1)
Ceq (mmol L-1)
C eq (mmol L-1)

9.1.5 Figure 5

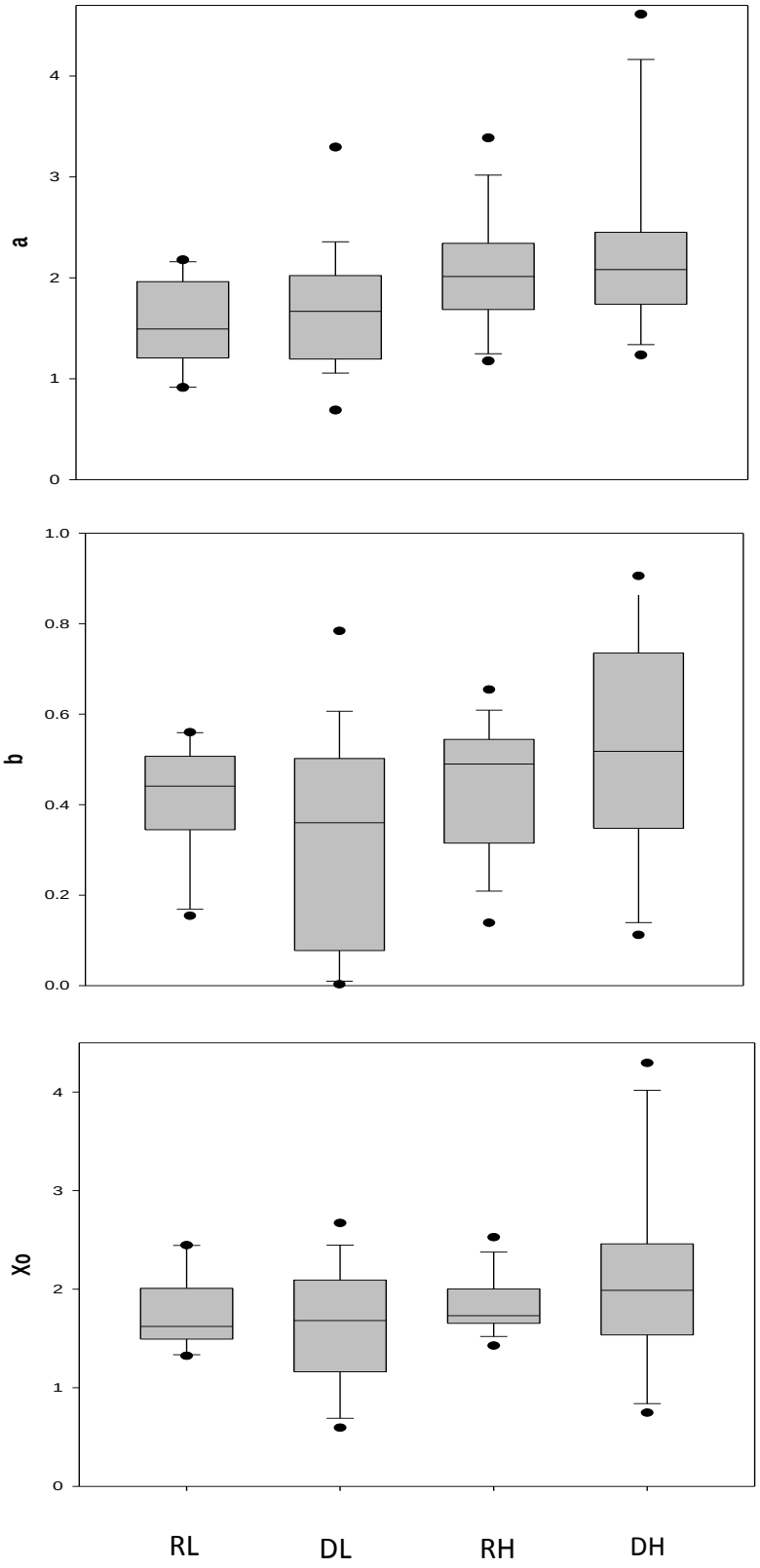

9.1.6 Table 1

	a	X_o	b
C	0.09	0.322**	0.279**
pH	-0.170	-0.381**	-0.24*
S_{CaPO4}	0.262*	0.081	0.036
Al_p	0.297**	0.175	0.320**
Al_o	0.417**	0.316**	0.375**
Al_d	0.291**	0.2	0.237*
Fe_p	0.33**	0.156	0.268**
Fe_o	0.275*	0.135	0.243*
Fe_d	0.235*	0.094	0.179
Mn_p	0.39**	0.421**	0.384**
Mn_o	0.4**	0.387**	0.518**
Mn_d	0.178	0.232*	0.16
Al_o/Al_d	-0.031	-0.071	-0.045
Fe_o/Fe_d	-0.148	-0.098	-0.033
Mn_o/Mn_d	0.34**	0.317**	0.174
depth	0.475**	0.143	0.129
elevation	0.25*	0.112	0.219

9.1.7 Table 2

	%C	pH	S_{CaPO4}	Al_p	Al_o	Al_d	Fe_p	Fe_o	Fe_d	Mn_p	Mn_o
%C	1										
pH	-0.636**	1									
S_{CaPO4}	-0.007	-0.061	1								
Al_p	0.285**	-0.209	0.217	1							
Al_o	0.566**	0.352**	0.308**	0.699**	1						
Al_d	0.401**	0.237**	0.065	0.355**	0.530**	1					
Fe_p	0.403**	-0.291*	0.266**	0.910**	0.745**	0.416	1				
Fe_o	0.504**	-0.224*	0.312**	0.580**	0.849**	0.439**	0.649**	1			
Fe_d	0.124	-0.081	0.183	0.212	0.184	0.681**	0.265*	0.181	1		
Mn_p	0.442**	-0.214	0.314**	0.372**	0.652**	0.299*	0.409**	0.494**	0.211	1	
Mn_o	0.320**	-0.134	0.129	0.496**	0.496**	0.359**	0.22	0.330**	0.317*	0.817**	1
Mn_d	0.217	-0.33**	-0.019	0.104	0.358**	0.480**	0.145	0.246*	0.343**	0.486**	0.531**

9.1.8 Table 3

	RL	DL	RH	DH
%C	0.62 (0.32,0.86)	0.48 (0.35,0.83)	0.99 (0.56,1.99)	1.63 (1.41,2.22)
pH	5.3 (5.25,5.49)	5.37 (5.25,5.49)	5.11 (4.91,5.22)	5.01 (5.02,5.22)
Al_p	0.66 (0.52, 0.82)	0.55 (0.41, 0.79)	0.9 (0.62,1.22)	1.03 (0.83,1.25)
Al_o	0.49 (0.42,0.49)	0.35 (0.28,0.39)	0.33 (0.44, 0.7)	0.77 (0.58, 0.93)
Al_d	0.86 (0.55,0.94)	0.72 (0.61,0.93)	0.86 (0.84,1.49)	1.17 (0.92,1.45)
Fe_p	0.62 (0.31,0.56)	0.41 (0.36,0.62)	0.75 (0.52,0.91)	0.81 (0.69,0.99)
Fe_o	0.61 (0.43, 0.66)	0.4 (0.26, 0.46)	0.59 (0.46, 1.03)	1 (0.81, 1.24)
Fe_d	3.23 (2.42,3.57)	2.8 (2.37,3.12)	3.69 (2.58,4.06)	3.55 (2.70,3.97)
Mn_p	0.0099 (0.0081,0.0114)	0.0065 (0.0033,0.0127)	0.0099 (0.0071,0.0181)	0.0149 (0.0087,0.0207)
Mn_o	0.0254 (0.0193,0.0429)	0.0085 (0.0067,0.2377)	0.0454 (0.0186,0.0516)	0.0502 (0.0188,0.0646)
Mn_d	0.0543 (0.0258,0.0684)	0.0362 (0.0187,0.0648)	0.0838 (0.0301,0.1124)	0.0733 (0.0335,0.1036)
Si_o	0.03 (0.02,0.03)	0.02 (0.01,0.02)	0.03 (0.03,0.04)	0.04 (0.03,0.04)
Fe_o/Fe_d	0.19 (0.14,0.2)	0.14 (0.08,0.2)	0.21 (0.13,0.29)	0.32 (0.21,0.39)
Al_o/Al_d	0.56 (0.47,0.99)	0.48 (0.34,0.53)	0.57 (0.39,0.75)	0.74 (0.44,0.92)

9.1.9 Table 4a.

		ppm (mg/kg)							mg/100g	%									
Series	Horizon	P	K	Ca	Mg	Zn	Mn	Cu	Fe	B	CEC	Acidity	BaseSat	CaSat	MgSat	Ksat	N	C	CNRatio	pH	pHbase
Cu	A	7	45	291	39	1.5	101.4	0.6	28.2	0.2	6.5	68.5	31.5	22.3	5	1.8	0.39	6.6	17.96	4.8	5.58
Cu	B	3	29	61	29	0.6	15.1	0.8	26.4	0.1	3.9	83	17	9.3	5.1	2	0.1	1.7	19.21	5.15	5.86
Ed	A	7	50	122	32	1.1	62.2	0.7	26.7	0.2	6.4	84.1	15.9	9.8	4	2	0.33	6	16.96	4.72	5.59
Ed	B	2	36	66	30.5	0.55	12.65	0.8	31.9	0.1	4.1	83.7	16.3	8.95	5.75	2.1	0.04	0.8	22.05	5.13	5.85
Pw	A	7	65	192	46	1.7	78.8	0.5	40.2	0.2	7.5	85.4	14.6	9.5	3.7	1.5	0.42	7.1	15.07	4.42	5.32
Pw	B	4	26	52	20	0.5	28.3	0.8	34.8	0.1	3.8	81.2	18.8	9.6	4.3	1.7	0.13	2.7	15.87	4.96	5.86
Rk	A	8.5	61.5	111.5	32.5	2.15	51	0.6	35.2	0.2	7.45	86.6	13.4	7.5	3.4	2.15	0.37	8.8	21.95	4.655	5.31
Rk	B	2	34	47	47	0.9	18.5	0.7	35.7	0.1	4.6	85.5	14.5	5.2	8.2	1.8	0.16	3.4	19.9	4.91	5.73

9.1.10 Table 4b.

		ppm (mg/kg)								mg/100g	%									
Series	Horizon	P	K	Ca	Mg	Zn	Mn	Cu	Fe	B	CEC	Acidity	BaseSat	CaSat	MgSat	Ksat	N	C	C:N	pH	pHbase
Cd	A	5.5	51.5	208	66	1.05	39.7	0.8	22.7	0.25	6.05	68.15	31.85	18.55	8	2.2	0.19	4.37	19.67	5.045	5.815
Cd	B	2	41.5	56	49	0.55	13.25	0.75	20.35	0.1	2.8	66.7	33.3	11.8	15.95	3.75	0.03	0.78	24.78	5.48	6.09
Cu	A	5	43	468	75	1.1	70.7	0.6	22.5	0.2	7.2	57.8	42.2	31.6	10.8	2.3	0.2	3.54	17.63	5.13	5.84
Cu	B	2	42	68	35	0.4	13.7	0.7	24.3	0.1	3.7	78.3	21.7	10	7.3	3	0.02	0.53	22.28	5.305	5.955
Fa	A	6	59.5	174	43	1.4	18.55	0.6	55.75	0.2	6.25	82.7	17.3	10.65	4.75	2.45	0.2	4.37	22.98	4.86	5.675
Fa	B	2	39	48	58	0.4	6.8	0.6	22.5	0.1	3.6	76.6	23.4	7.2	13.7	3.7	0.02	0.48	21.6	5.3	5.95

9.1.11 Table 5

Lower															
	A-horizon	S	4.935	0.229	5.177	23.31	5.36	0.6188	0.487	0.0091	0.5368	0.6195	0.01729	0.83404	2.4027	0.0353
		B	5.13	0.161	3.647	21.01	4.83	0.4954	0.353	0.0144	0.5174	0.7046	0.03108	0.69183	2.06494	0.0334
		F	4.91	0.22	3.83	17.38	3.79	0.6044	0.482	0.0179	0.464	0.56	0.03843	0.70392	2.87901	0.05937
		T	5.215	0.184	3.447	17.88	10.8	0.5696	0.55	0.0293	0.8039	0.5065	0.10565	1.20867	2.75671	0.10844
	B-Horizon	S	5.335	0.024	0.533	22.56	3.15	0.5766	0.416	0.0058	0.3205	0.3881	0.00697	0.63751	3.60896	0.04193
		B	5.37	0.021	0.649	24.78	3.05	0.4571	0.372	0.0065	0.3261	0.3777	0.02035	0.51833	2.69552	0.02922
		T	5.27	0.032	0.674	23.9	4.13	0.5811	0.463	0.0243	0.5013	0.4034	0.03061	0.50329	2.54382	0.04148
		F	5.31	0.023	0.375	16.54	5.7	0.8142	0.567	0.0085	0.4399	0.494	0.03846	0.64983	3.86276	0.05823
Upper																
	A-horizon	S	4.575	0.342	6.685	19.01	5.05	1.0944	1.048	0.0223	0.8299	0.9021	0.02628	1.30988	3.08369	0.04161
		B	4.66	0.37	7.158	17.82	4.58	1.2135	1.027	0.0367	0.9402	0.9514	0.05142	1.36632	3.60509	0.09229
		F	4.66	0.373	6.982	19.23	5.02	1.141	0.822	0.0275	1.0782	1.1994	0.0559	1.23556	2.82955	0.0885
		T	4.73	0.411	6.79	15.08	2.3	0.9098	0.93	0.0463	0.8306	0.9868	0.06952	1.1132	3.49978	0.07292
	B-Horizon	S	5.11	0.125	1.986	17.99	2.42	1.1963	0.846	0.0108	0.7114	1.0313	0.01664	1.14112	5.05731	0.02765
		B	5.08	0.056	1.405	21.38	5.75	1.0482	0.823	0.0183	0.648	0.8321	0.02686	0.96358	4.04354	0.03725
		T	5.15	0.068	1.422	18.37	6.12	1.0087	0.888	0.0153	0.5685	0.85	0.04957	0.9833	3.45287	0.07934
		F	4.9	0.102	1.819	20.05	8.2	1.1842	1.096	0.0182	0.6963	1.113	0.04637	1.16401	4.94147	0.08511

9.1.12 Table 6

	local element	pH	%N	%C	C:N	S	Al_p	Fe_p	Mn_p	Al_o	Fe_o	Mn_o	Al_d	Fe_d	Mn_d
A- horizons	**ss**	4.74	0.3592148	6.79033	16.648646	6.333	0.9601309	0.9729	0.02656	0.7351	1.0448	0.0389	1.1132	3.7248	0.0543
	sv	4.64	0.358068	6.01638	17.878345	7.295	1.041846	0.7313	0.02588	0.7839	0.671	0.0294	1.48255	3.6076	0.1457
	sx	4.73	0.290439	5.95026	19.066688	4.199	0.7155566	0.5508	0.01513	0.5773	0.8953	0.0239	0.79421	2.4841	0.0353
	vv	4.74	0.3626677	6.22655	18.339956	3.671	0.724017	0.585	0.02708	1.0169	1.0934	0.064	1.15524	2.879	0.0885
	xs	4.83	0.3320096	5.90818	16.964911	3.072	1.101384	1.0553	0.05351	0.9737	0.9432	0.0828	1.24081	3.4629	0.1076
	xx	4.86	0.1568759	3.64663	21.280764	5.361	0.6241302	0.529	0.01659	0.5533	0.667	0.0376	0.77359	2.2261	0.0391
B- Horizons	**ss**	5.055	0.0720255	1.45617	21.774393	4.173	0.9345235	0.7806	0.01941	0.5676	0.9754	0.0573	1.04401	3.531	0.0394
	sv	5.18	0.0277403	0.82569	20.614031	7.137	0.8514587	0.5979	0.01836	0.5424	0.6475	0.0232	0.904	3.929	0.0364
	sx	5.295	0.0322859	0.70635	17.264001	5.306	0.8293905	0.5853	0.00948	0.4486	0.6535	0.0176	0.78793	4.0934	0.048
	vv	5.27	0.0511704	0.9141	20.487901	4.066	0.5868396	0.4795	0.0182	0.532	0.4439	0.0464	0.83057	3.6016	0.0714
	xs	5.115	0.0451816	0.85169	18.621692	5.748	0.9914727	0.7811	0.01373	0.4711	0.5432	0.0475	0.84016	3.7053	0.0623
	xx	5.335	0.0228037	0.53305	23.360808	3.782	0.450993	0.3382	0.0062	0.3571	0.4153	0.0204	0.58716	2.9706	0.0292